How convective parameterization and Cloud microphysics affect climate simulation?
- sub-seasonal to decal variability -

Young-Min Yang and Bin Wang

IPRC, University of Hawaii at Manoa
ESMC, NUIST

"Subseasonal to Seasonal climate forecast will be widely used a decade from now as weather forecasts are today."

Subseasonal forecast on a time scale of 2-8 weeks has immense social-economic benefits for hazard prevention, risk management, economic planning, and shaping policy decision making.

SOURCE: Modified from the Earth System Prediction Capability Office.

Source: "Next Generation Earth System Prediction: Strategies for Subseasonal to Seasonal Forecasts" NAS report 2016

Convective parameterization

- **Cloud budget equation for** $\varepsilon, h_u(T_{vu}), q_t(l_u)$

$$\frac{\partial \eta}{\partial z} = (\varepsilon - \delta)\eta$$

$$\frac{\partial h_u}{\partial z} = -\varepsilon\left(h_u - \bar{h}\right) + S_h$$

$$\frac{\partial q_t}{\partial z} = -\varepsilon(q_t - \bar{q}) + S_{q_t}$$

S_h, S_{q_t}: source/sink term

$S_{q_t} = c l_u$

Entrainment rate

Initiation of convection

Cloud microphysics : conversion rate of cloud water to rainfall

Closure (cloud base mass flux)

ε, δ : entrainment / detrainment rate
h_u : moist static energy (MSE) of updraft
q_t : total water of updraft
q_u : water vapor of updraft
l_u : liquid water of updraft
L_c : coefficient of latent heat
$\overline{q^*}$: grid mean saturated specific humidity
$\overline{h^*}$: grid mean saturated MSE
l_u : liquid water of updraft
T_{vu}: virtual temperature of updraft
g: gravity
z : height
c : conversion ratio of cloud liquid water to rain drop
zt = height at cloud top

Cloud Resolving Model

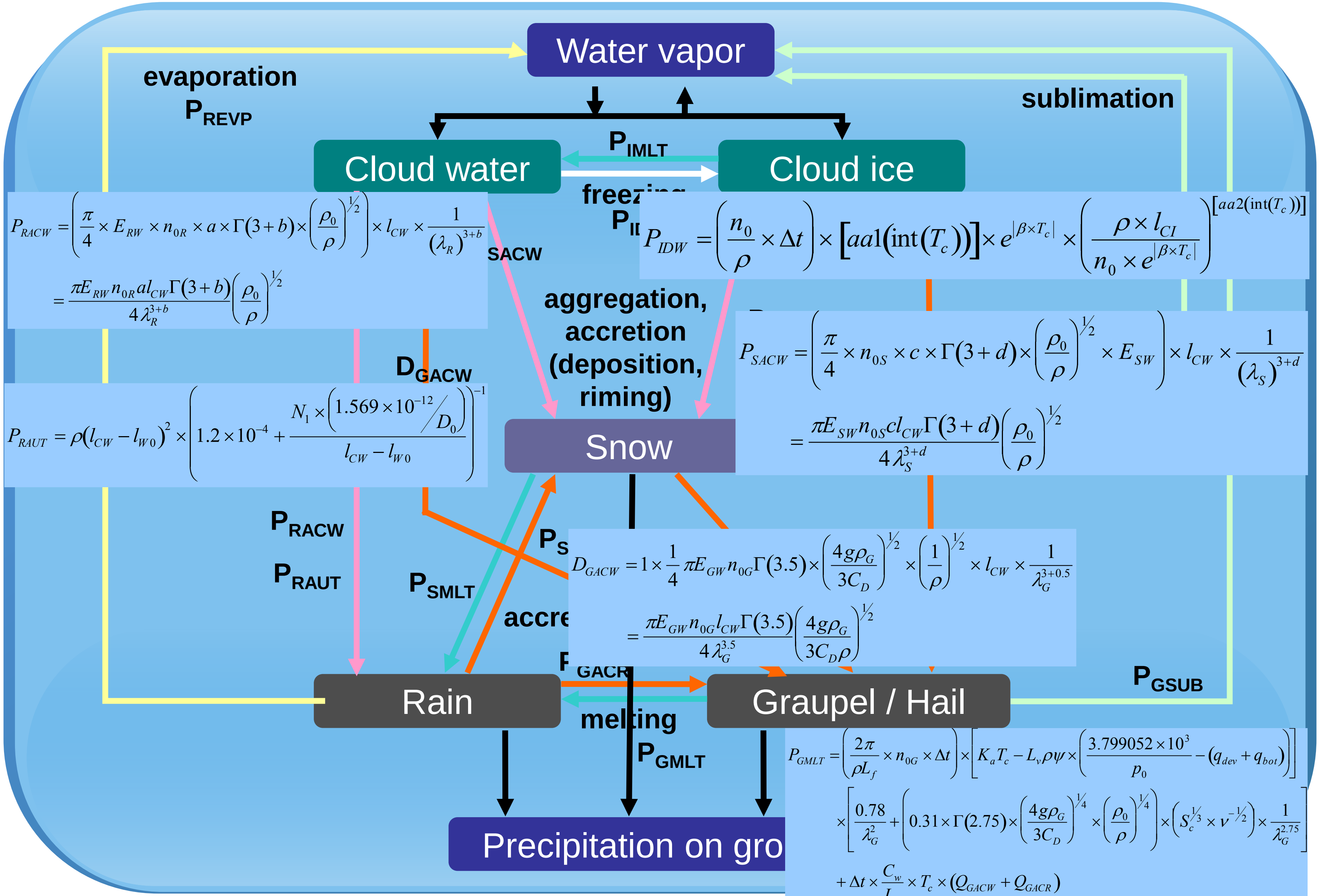

$$P_{RACW}=\left(\frac{\pi}{4}\times E_{RW}\times n_{0R}\times a\times\Gamma(3+b)\times\left(\frac{\rho_0}{\rho}\right)^{1/2}\right)\times l_{CW}\times\frac{1}{(\lambda_R)^{3+b}}=\frac{\pi E_{RW}n_{0R}al_{CW}\Gamma(3+b)}{4\lambda_R^{3+b}}\left(\frac{\rho_0}{\rho}\right)^{1/2}$$

$$P_{RAUT}=\rho(l_{CW}-l_{W0})^2\times\left(1.2\times10^{-4}+\frac{N_1\times\left(1.569\times10^{-12}/D_0\right)}{l_{CW}-l_{W0}}\right)^{-1}$$

$$P_{IDW}=\left(\frac{n_0}{\rho}\times\Delta t\right)\times\left[aa1(\mathrm{int}(T_c))\right]\times e^{|\beta\times T_c|}\times\left(\frac{\rho\times l_{CI}}{n_0\times e^{|\beta\times T_c|}}\right)^{[aa2(\mathrm{int}(T_c))]}$$

$$P_{SACW}=\left(\frac{\pi}{4}\times n_{0S}\times c\times\Gamma(3+d)\times\left(\frac{\rho_0}{\rho}\right)^{1/2}\times E_{SW}\right)\times l_{CW}\times\frac{1}{(\lambda_S)^{3+d}}=\frac{\pi E_{SW}n_{0S}cl_{CW}\Gamma(3+d)}{4\lambda_S^{3+d}}\left(\frac{\rho_0}{\rho}\right)^{1/2}$$

$$D_{GACW}=1\times\frac{1}{4}\pi E_{GW}n_{0G}\Gamma(3.5)\times\left(\frac{4g\rho_G}{3C_D}\right)^{1/2}\times\left(\frac{1}{\rho}\right)^{1/2}\times l_{CW}\times\frac{1}{\lambda_G^{3+0.5}}=\frac{\pi E_{GW}n_{0G}l_{CW}\Gamma(3.5)}{4\lambda_G^{3.5}}\left(\frac{4g\rho_G}{3C_D\rho}\right)^{1/2}$$

$$P_{GMLT}=\left(\frac{2\pi}{\rho L_f}\times n_{0G}\times\Delta t\right)\times\left[K_aT_c-L_v\rho\psi\times\left(\frac{3.799052\times10^3}{p_0}-(q_{dev}+q_{bot})\right)\right]\times\left[\frac{0.78}{\lambda_G^2}+\left(0.31\times\Gamma(2.75)\times\left(\frac{4g\rho_G}{3C_D}\right)^{1/4}\times\left(\frac{\rho_0}{\rho}\right)^{1/4}\right)\times\left(S_c^{1/3}\times\nu^{-1/2}\right)\times\frac{1}{\lambda_G^{2.75}}\right]+\Delta t\times\frac{C_w}{L_f}\times T_c\times(Q_{GACW}+Q_{GACR})$$

Budget of microphysical processes

(a)Light precipitation (0 – 10 mm day^{-1})

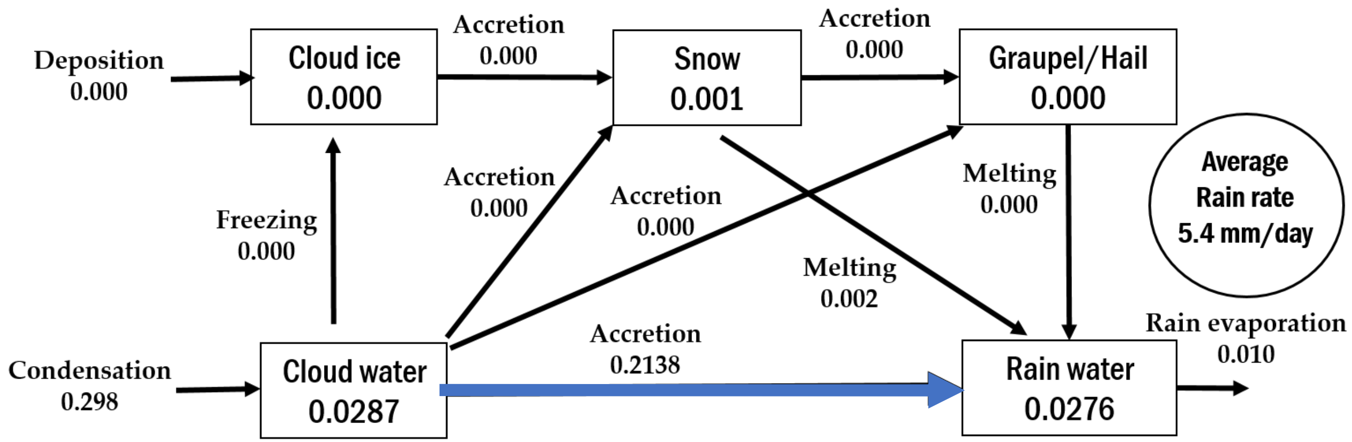

<Unit>

Cloud species : g/g

Processes : g/g/s

(b) Heavy precipitation (> 60 mm day^{-1})

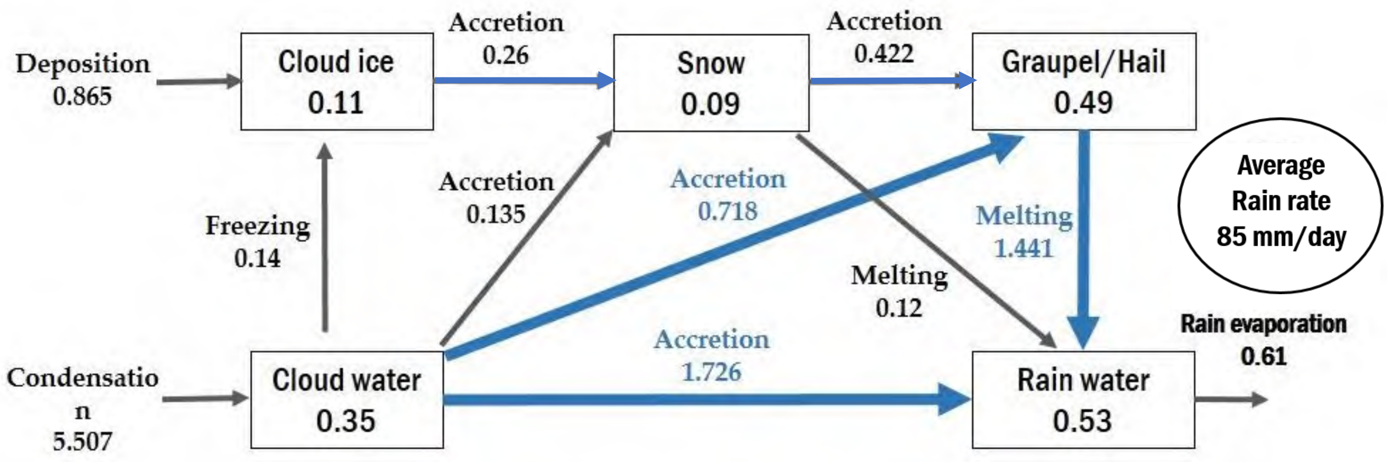

Experiment design

Exp.	Convective parameterization	Modified scheme
CTL	Tiedtke scheme (Tiedtke, 1989)	-
TRG	Tiedtke scheme (Tiedtke, 1989)	BL depth-dependent convective trigger function
ENT	Tiedtke scheme (Tiedtke, 1989)	Increased entrainment for deep convection
CMP	Tiedtke scheme (Tiedtke, 1989)	Reduced conversion rate of cloud water to rainfall
MOD	Tiedtke scheme (Tiedtke, 1989)	TRG+ENT+CMP

- 1990's fixed forcing
- NESMv3-SR
- 50yr integrations are used for analysis

NUIST-ESM V3

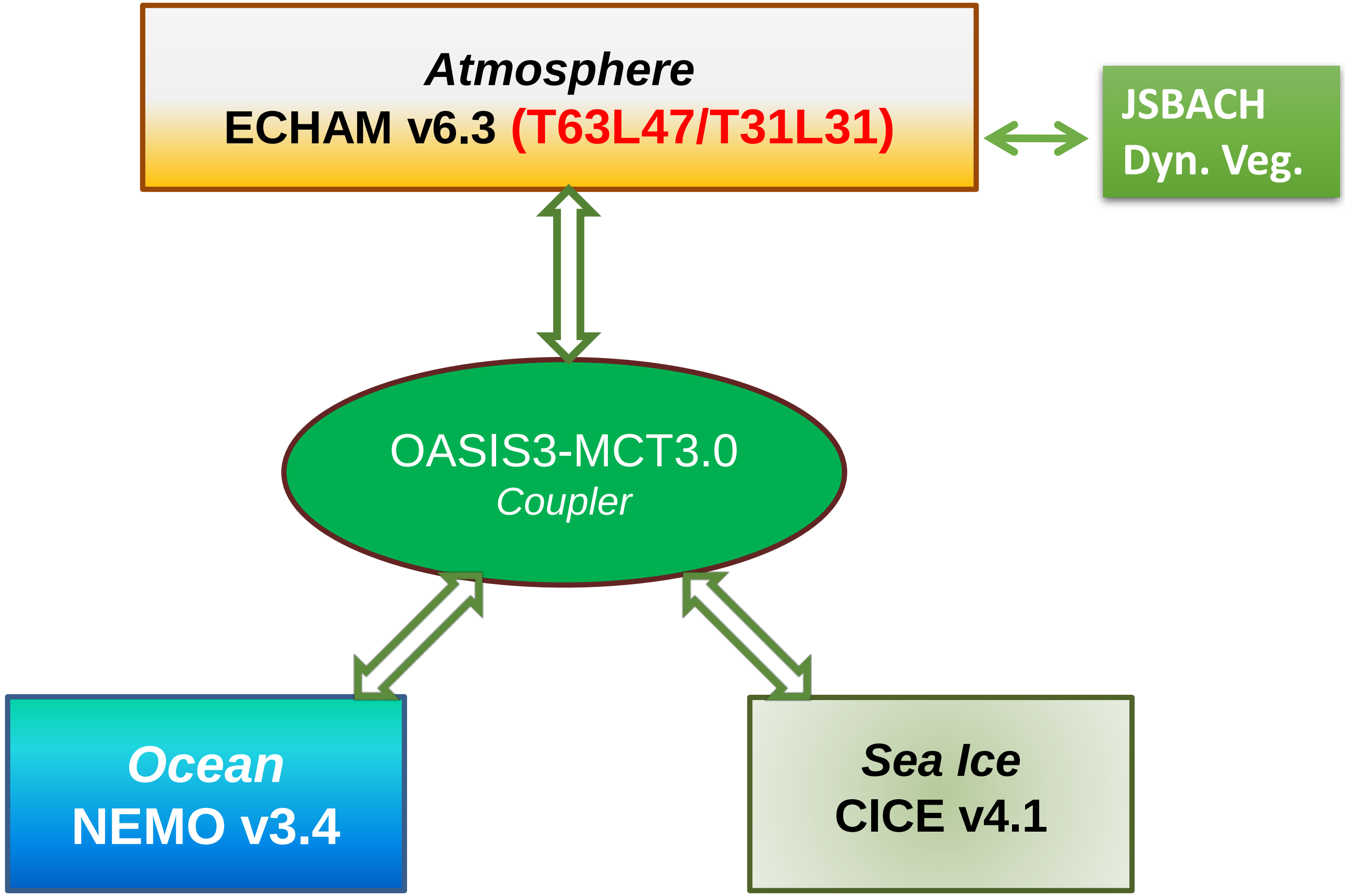

Dec. 2016

Cao, Wang, Yang et al. 2015, 2017

Correlation map of Land precipitation, SSTA and 850 hPa wind anomalies wrt DJF Nino-3.4 SSTA

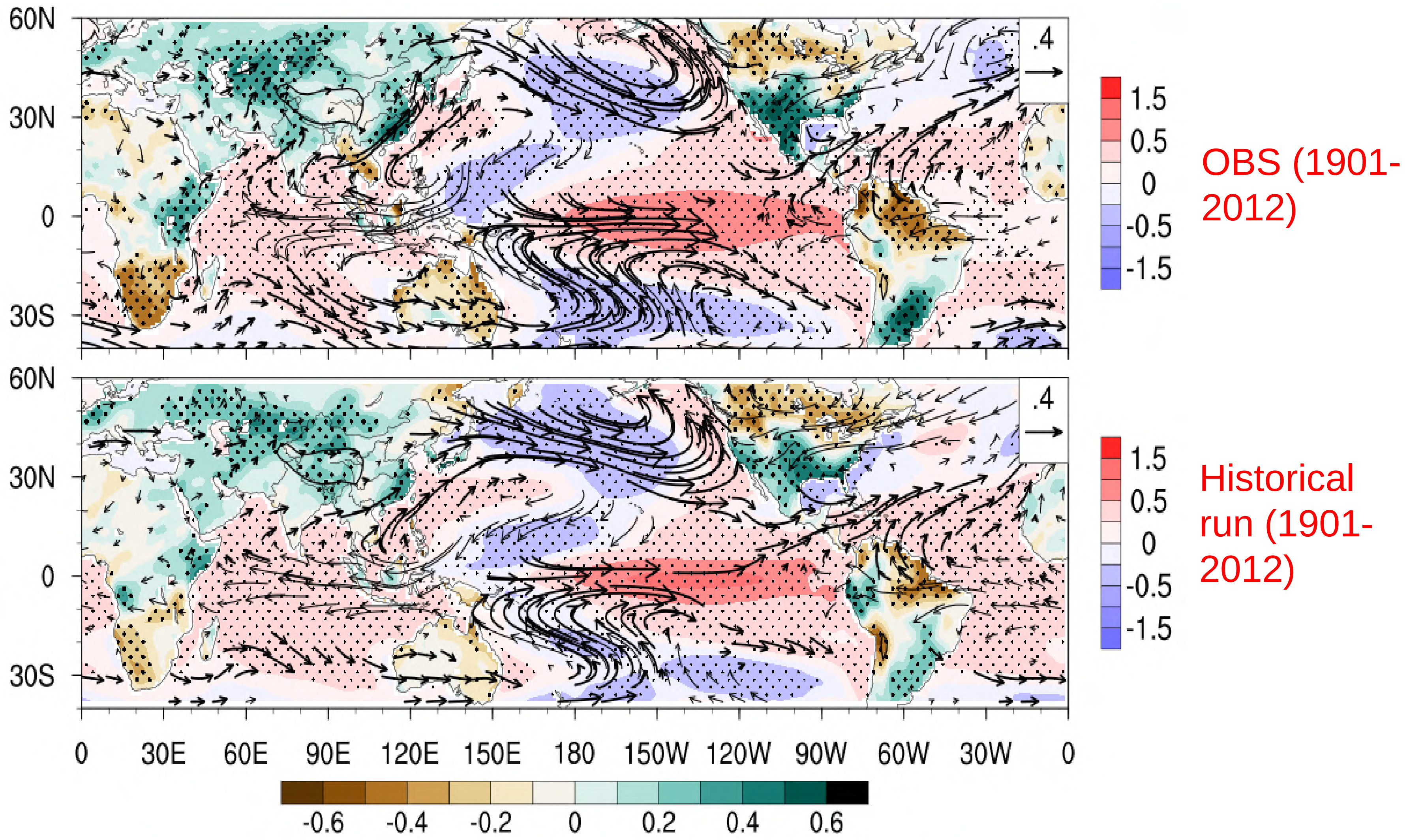

This talk discusses these issues

1) **Sub-seasonal**
"Improving MJO simulation by enhancing lower tropospheric heating - boundary layer convergence feedback"

2) **Seasonal**
"Sensitivity of moist physical parameterization on East Asia monsoon "
- seasonal evalution, large-scale circulation and ENSO-monsoon relationship"

3) **Interannual**
"Impact of convective parapmeterization on ENSO variability : role of atmospheric feedback"

4) **Inter-decal**
" How convective parameterization affect global warming slowdown? role of atmosphere heating and circulation"

“Improving MJO simulation by enhancing lower tropospheric heating - boundary layer convergence feedback”

Vertical Structure and Diabatic Processes of the MJO: *Global Model Evaluation Project*

MJO Task Force/YOTC and GASS 2012

Lag-regression of rainfall with Indian Ocean base point (70-90E; 5S-5N)

20-100day filtered

dash line – 5 m/s

Jiang et al. 2015

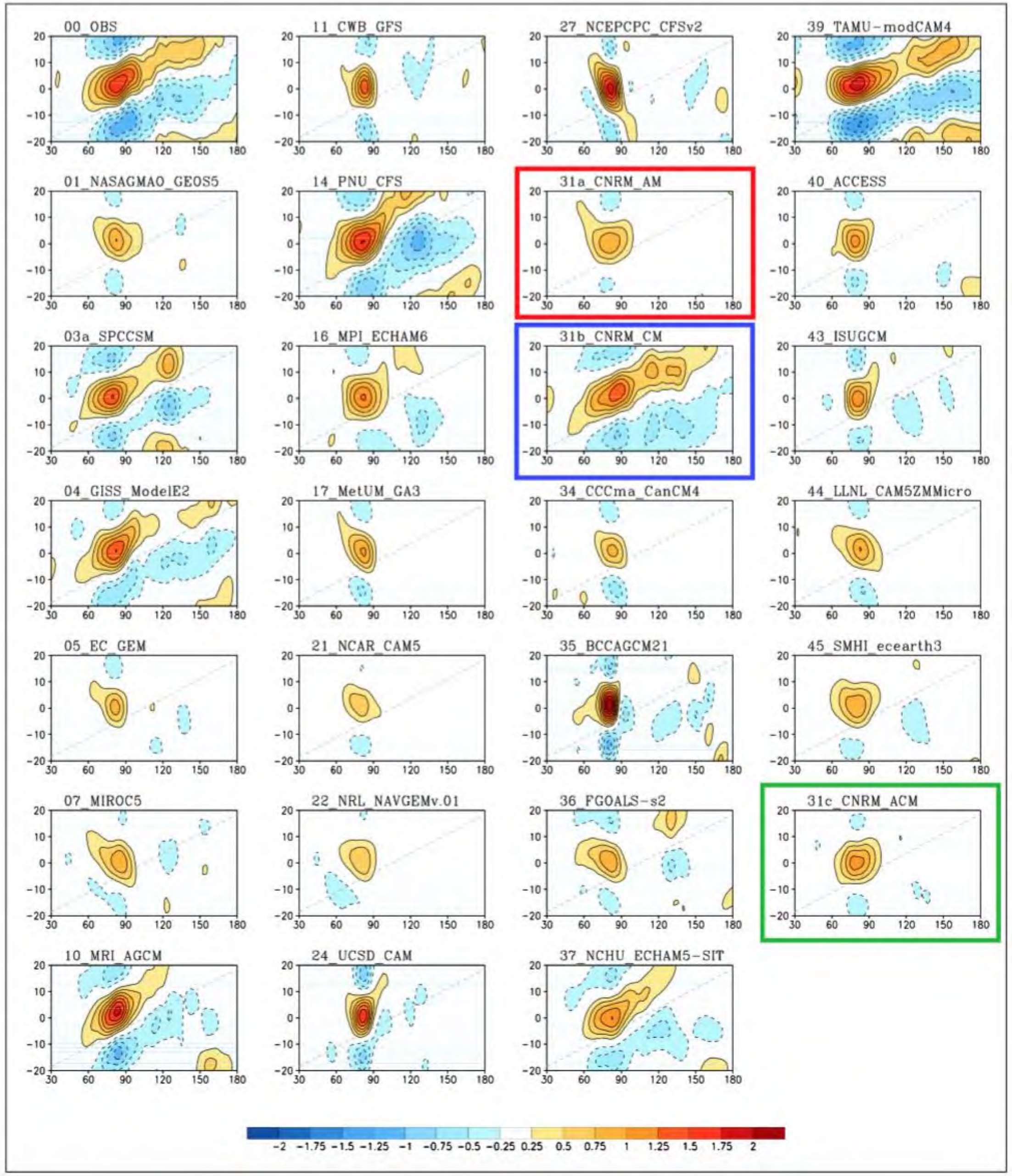

Experiments with modified convective parameterization schemes in the NUIST v3

Exp.	Convective parameterization	Modified scheme
CTL-TDK	Tiedtke scheme (Tiedtke, 1989)	-
TRG	Tiedtke scheme (Tiedtke, 1989)	BL depth-dependent convective trigger function (TRG)
SHC	Tiedtke scheme (Tiedtke, 1989)	Bottom-heavy diffusivity in shallow convection (SHC)
M-TDK	Tiedtke scheme (Tiedtke, 1989)	TRG + SHC
CTL-SAS	Simplified Arakawa-Schubert scheme (Lee et al. 2001)	-
M-SAS	Simplified Arakawa-Schubert scheme (Lee et al. 2001)	TRG +SHC

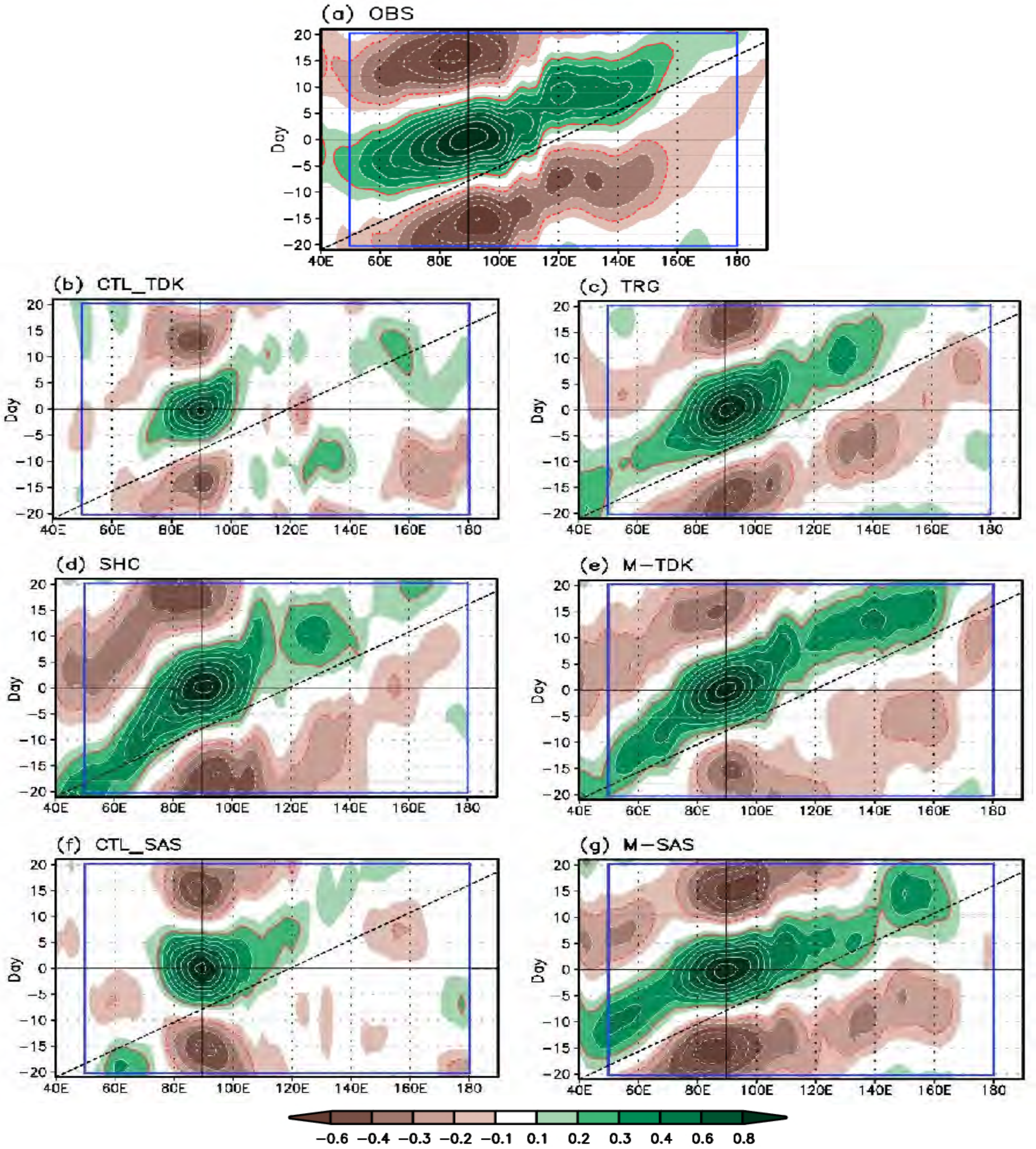

Improved eastward propagation

Figure 1. Propagation of MJO precipitation as depicted by the lead-lag correlation of 20-70 day filtered precipitation averaged over 10°S-10°N with reference to the precipitation at the MJO convective center over the equatorial Indian Ocean (10°S-10°N, 80°-100°E) during boreal winter (NDJFMA) derived from (a) observation and model simulations in the experiments of (b) CTL-TDK, (c) TRG, (d) SHC, (e) M-TDK, (f) CTL-SAS and (g) M-SAS. The red contour represents the correlation coefficient of ±0.2. Black dotted lines indicate eastward propagation speed of 5 m s^{-1}.

Improved Horizontal structure of diabatic heating at 700hPa

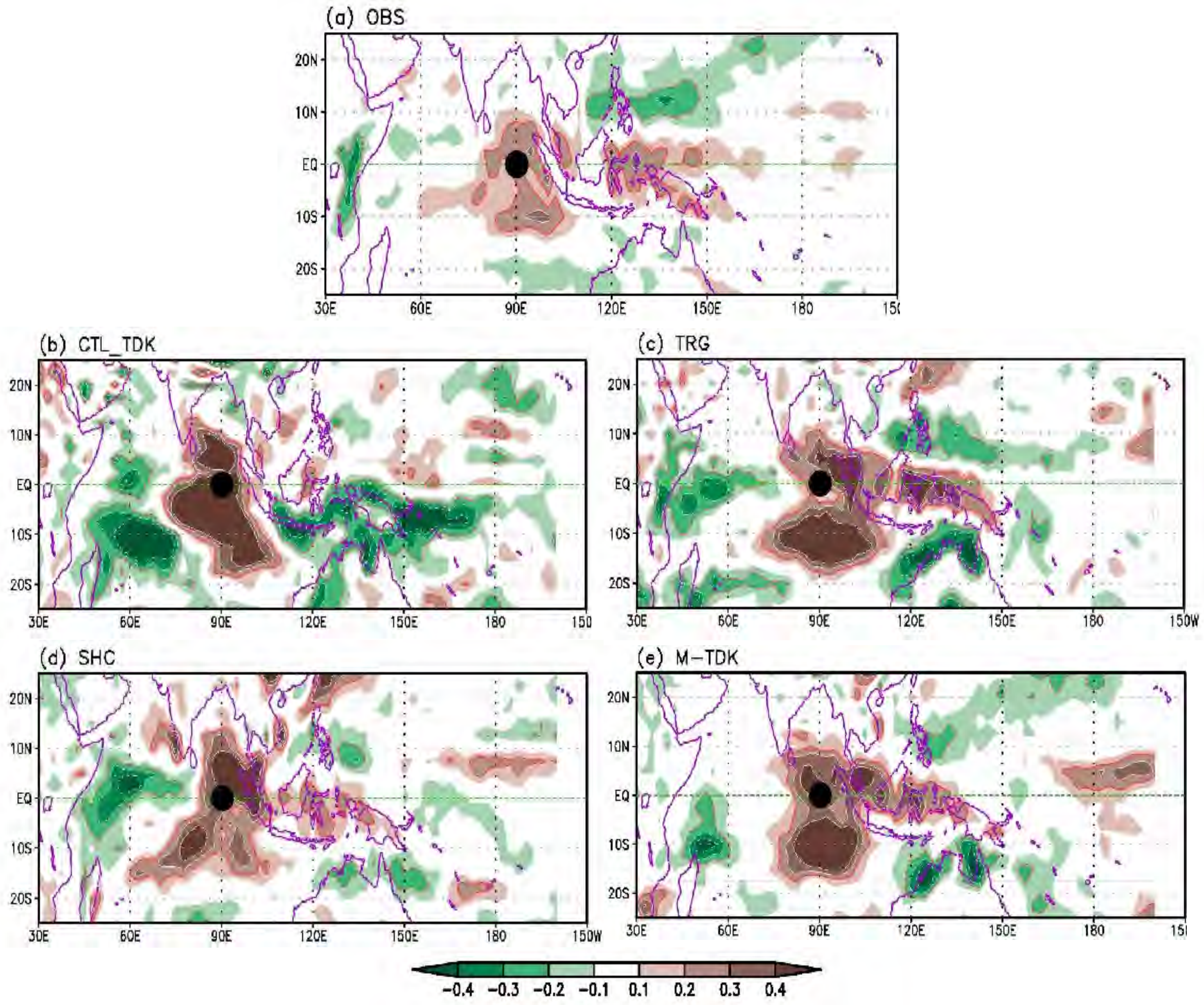

Improved BL moisture convergence

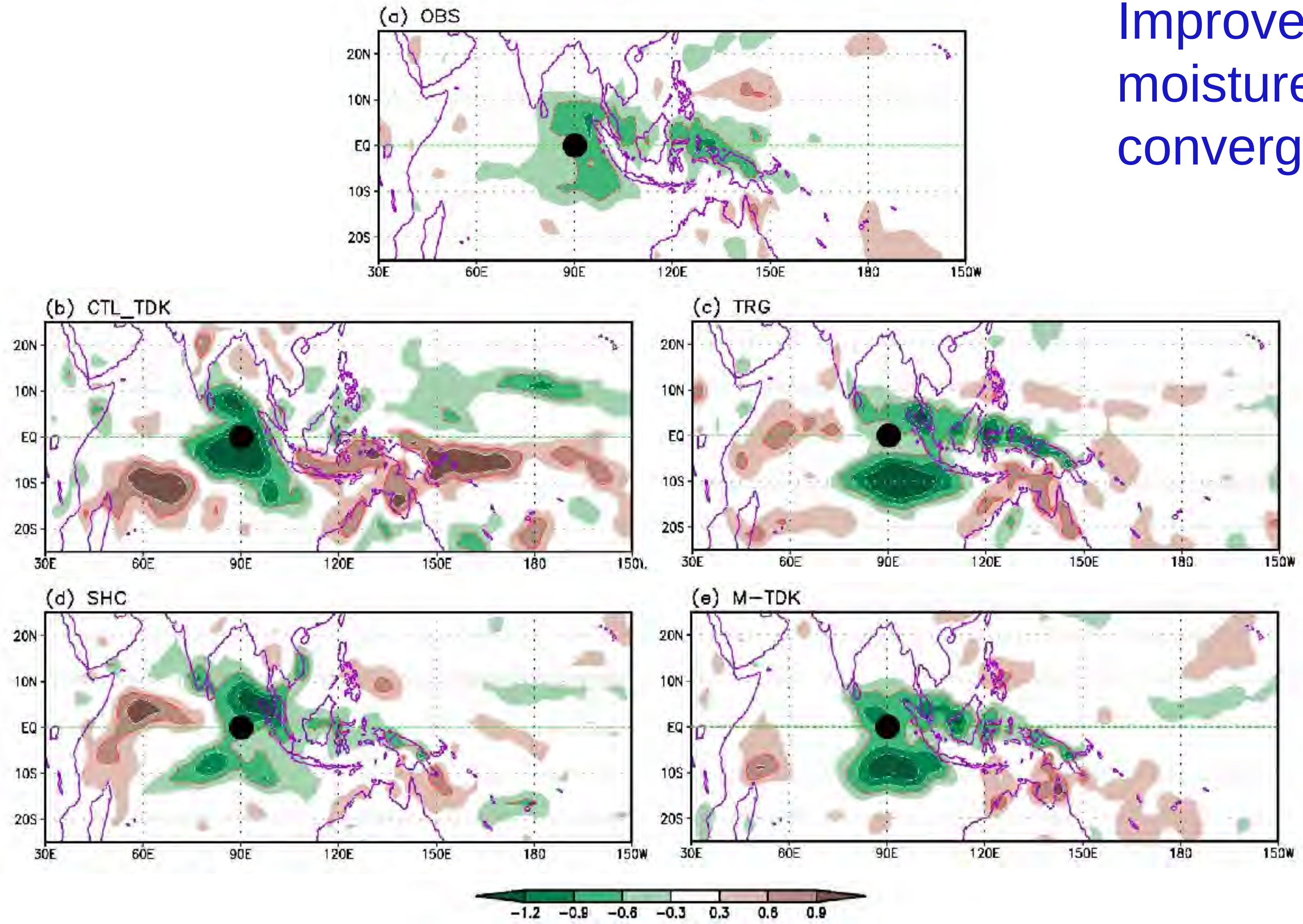

Improved Horizontal wind structure at 850hPa

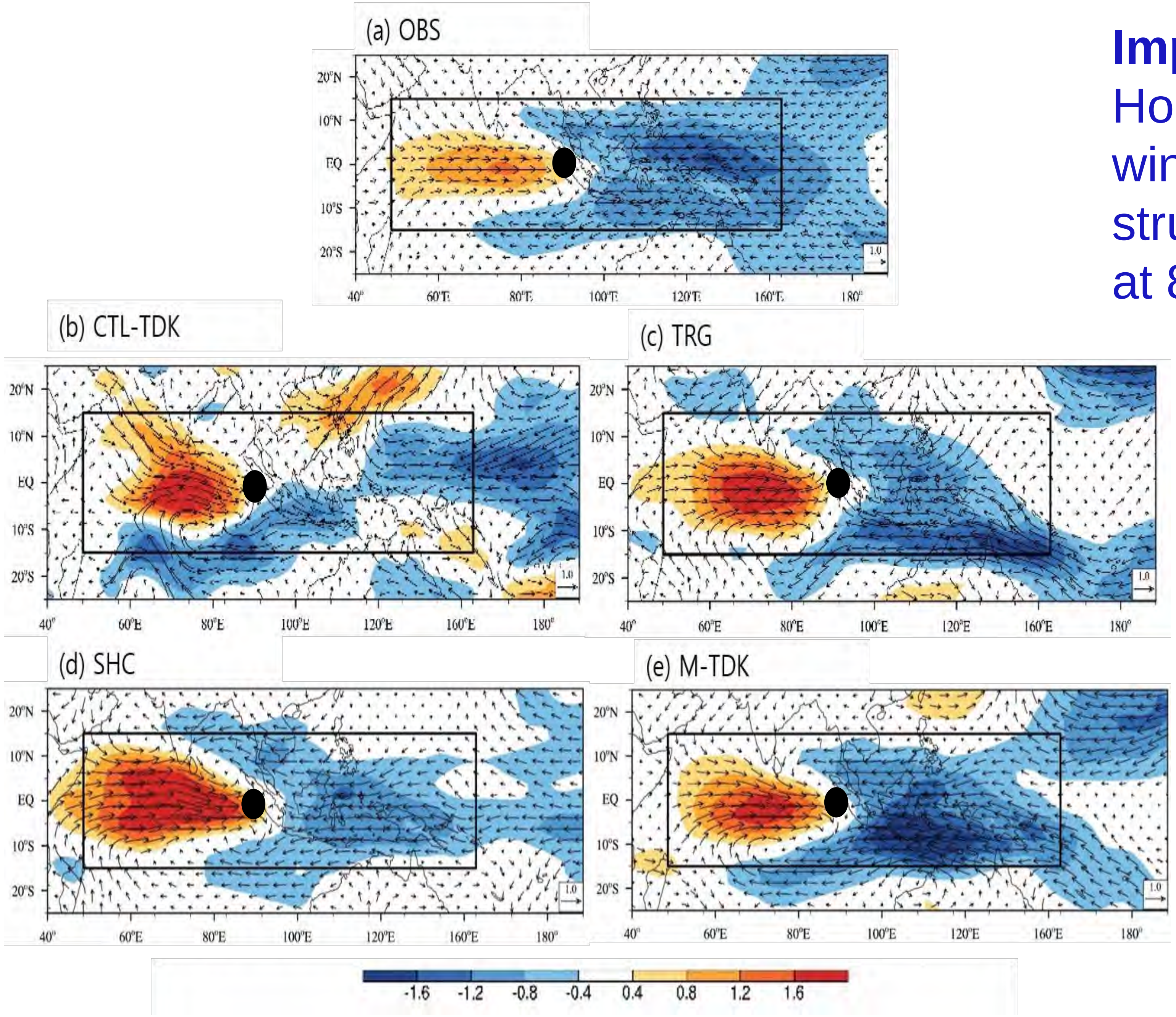

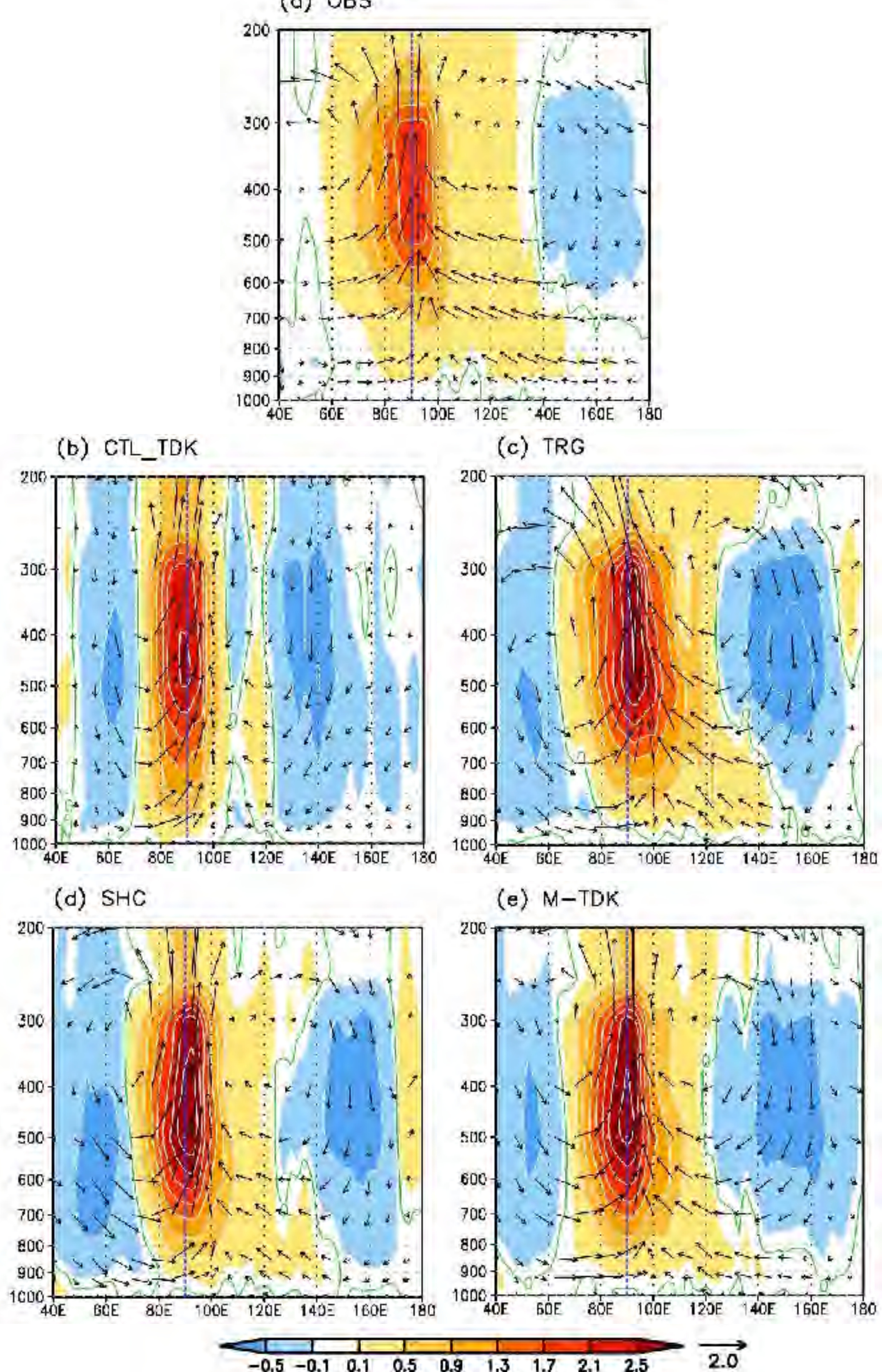

FIG.4 Equatorial zonal asymmetry in the diabatic heating (K day^{-1}, shading) and anomalous Walker cell (m s^{-1} for zonal wind and 0.01 Pa s^{-1} for the vertical velocity, vector) averaged between 5°S and 5°N in the observation (a) and model simulations (b)-(e). The structures in each panel are reconstructed using the same method as used in Fig. 3.

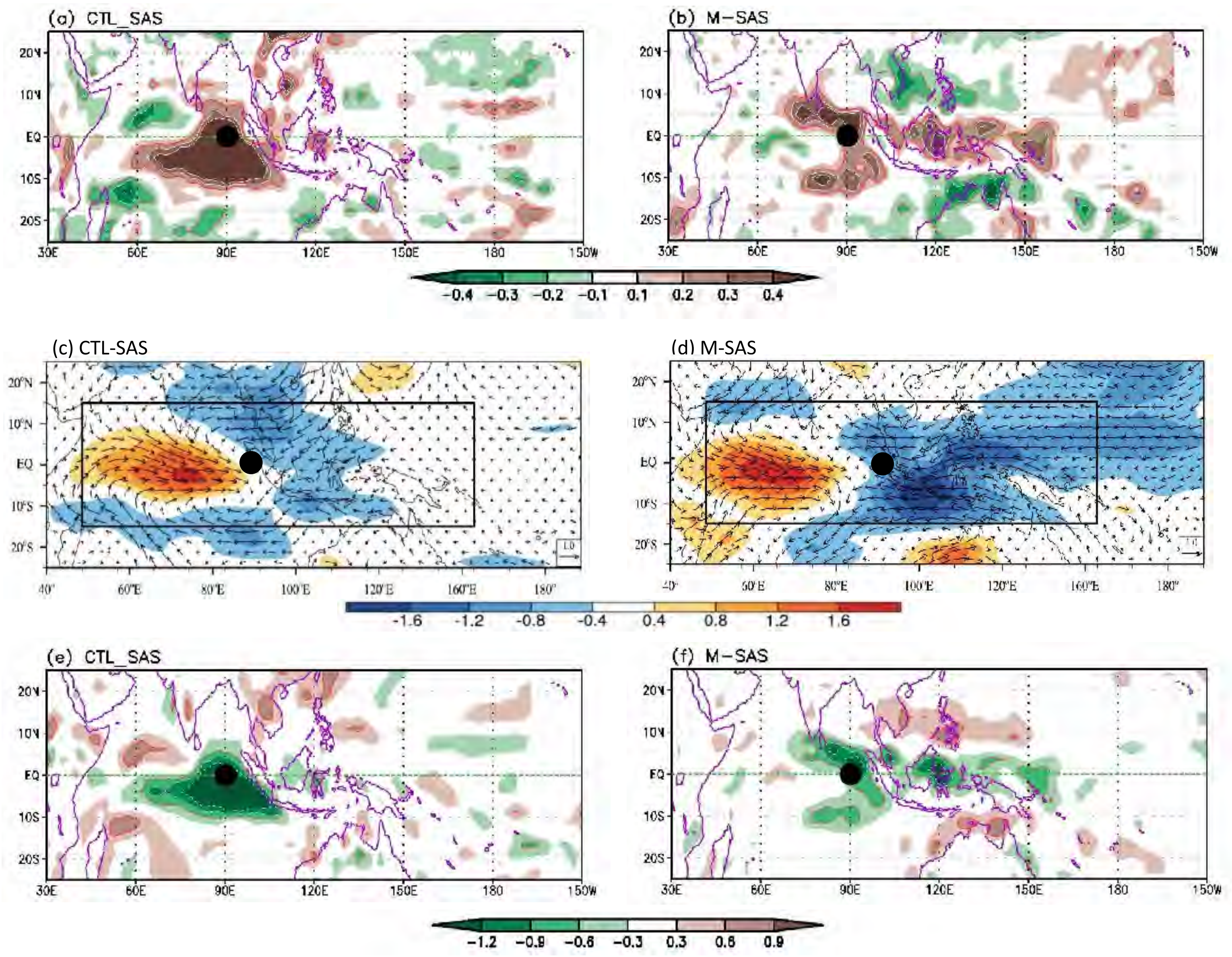

Fig. 10 Comparison of the dynamic structures simulated in CTL-SAS and M-SAS. (a) and (b) Horizontal structure of diabatic heating (K day^{-1}) at 700 hPa in C-SAS and M-SAS. (c) and (d) Horizontal structure of 850 hPa wind (m s^{-1}, vector) and 850 hPa zonal wind speed (U850) (m s^{-1}, shading) in C-SAS and M-SAS. (e) and (f) horizontal structure of boundary layer moisture convergence (day^{-1}) at 925 hP in C-SAS and M-SAS. The structures are regressed 20-70 day band pass filtered fields with reference to the MJO precipitation anomaly in the equatorial Indian Ocean (10S-10N, 80-100E), which is symbolized by the black filled circle. . The regression strengths are scaled to a fixed 3mm day^{-1} precipitation rate.

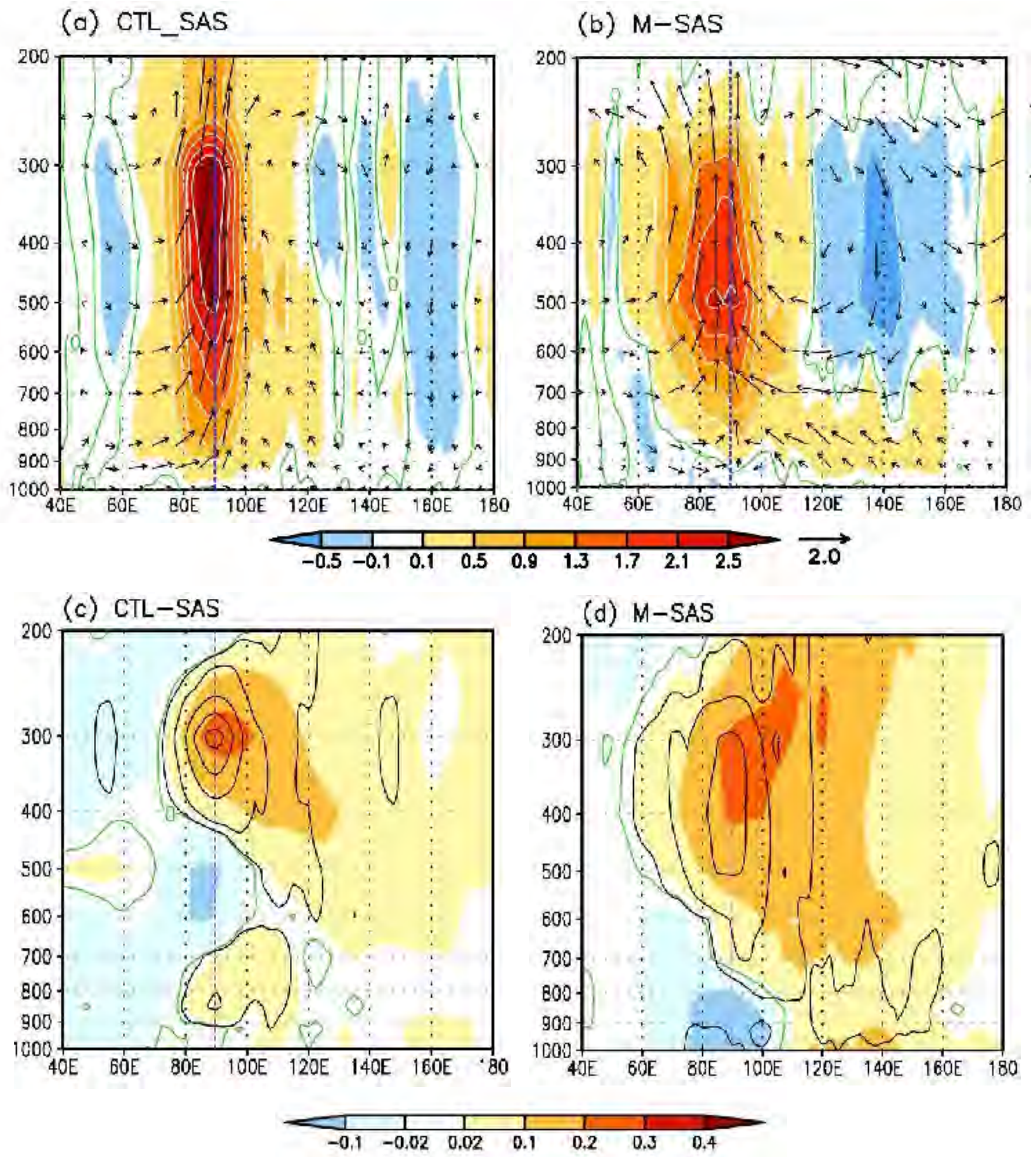

FIG.11 Comparison of the vertical structures simulated in CTL-SAS and M-SAS. (a) and (b) diabatic heating (K day^{-1}, shading) and anomalous Walker cell (m s^{-1} for zonal wind and 0.01 Pa s^{-1} for vertical velocity, vector) averaged between 5°S-5°N. (c) and (d) Eddy available potential energy (APE) generation rate (K^2 day^{-1}, contour) and temperature anomalies (K, shading) averaged between 5°S-5°N. The structures are regressed 20-70 day band pass filtered fields with reference to the precipitation anomaly in the equatorial Indian Ocean (10S-10N, 80-100E). The regression strengths are scaled to a fixed 3mm day^{-1} precipitation rate and averaged over 5S-5N. The intervals of contour in (c) and (d) are same as that of shading

Why MODIFICATIONS work

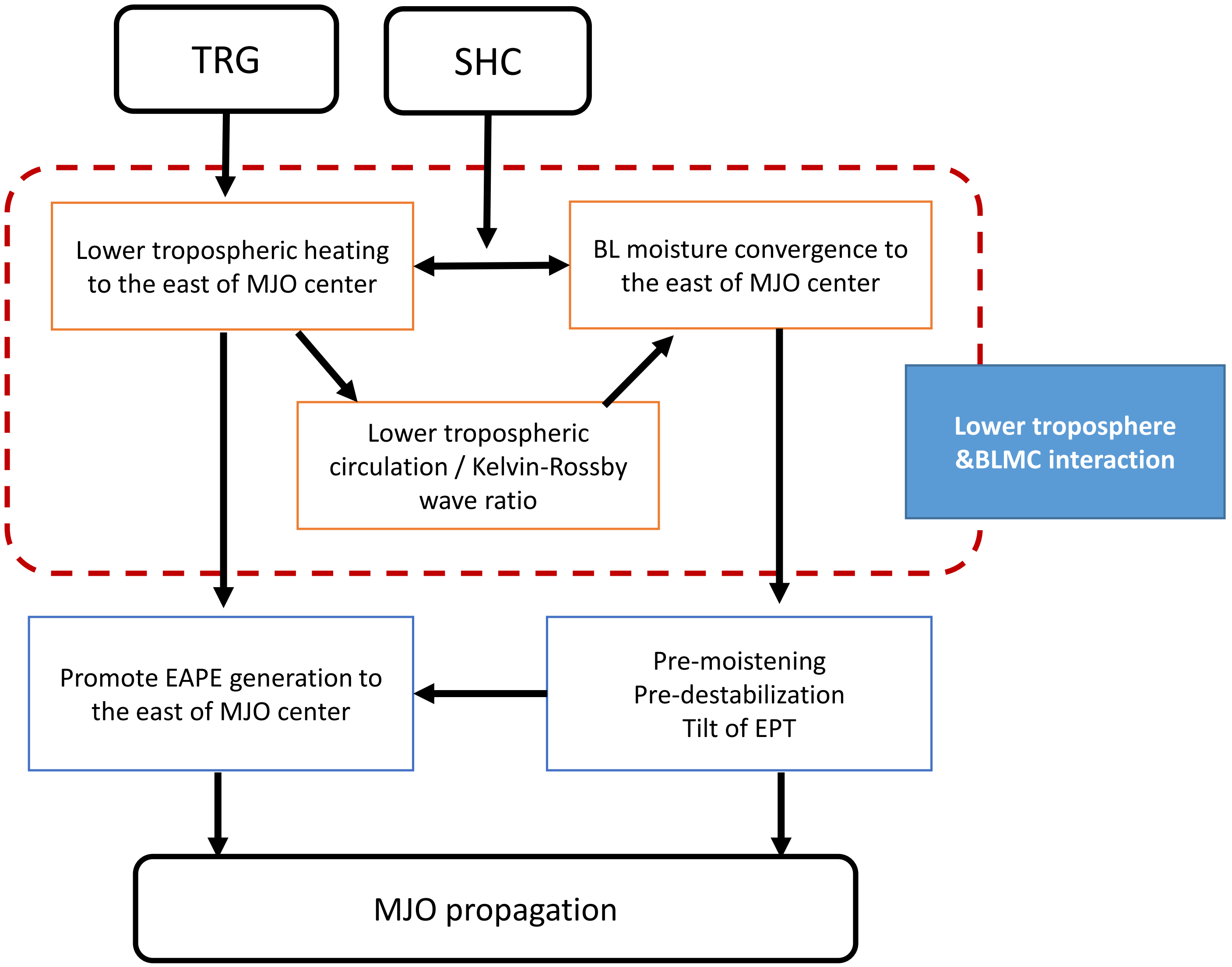

Mechanisms by which the modified cumulus schemes affect MJO structures and improve the MJO eastward propagation.

Summary

How to improve GCM simulation of MJO?

Modification of the convective parameterization schemes:
a) a BL depth-dependent convective trigger (TRG), and
b) a bottom-heavy diffusivity in the shallow convection scheme (SHC), aiming to enhance BLMC feedback on convection.

Results: In the NUIST-ESM, modified Tidtke (M-TDK) Simplified Arakawa-Schubert (M-SAS) convective schemes have significantly improved the quality of MJO simulation.

Why do the modification leads to improved simulation?

Implications: Correct simulation of the heating induced by shallow and/or congestus clouds and its interaction with BL dynamics is critical to realistic simulation of the MJO.

“Role of topography of Tibet on northward propagation”

- Does topography over Tibet affect northward propagation of precipitation?
- Using same model (M-TDK scheme)
- Decreasing topograhy : 100%, 75%, 50%, 25%, 0%
- Wind shear is critical for simulating northward propagation of precipitation

Lag correlation of Precipitation (Indian Ocean, Winter)

OBS

TOPO 100%

TOPO 80%

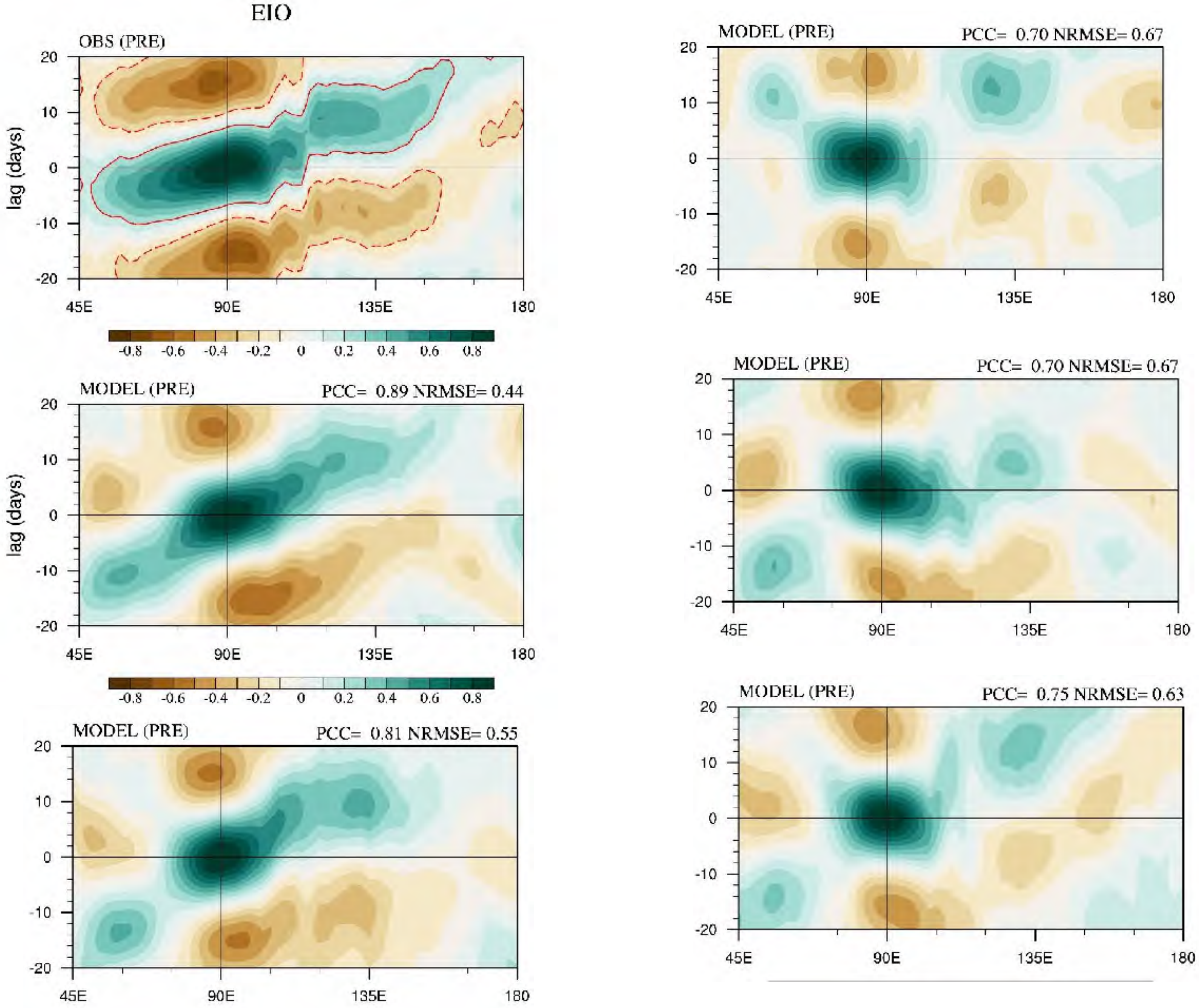

TOPO 50%

TOPO 20%

TOPO 0%

Lag correlation of precipitation (Indian ocean, Boreal summer)

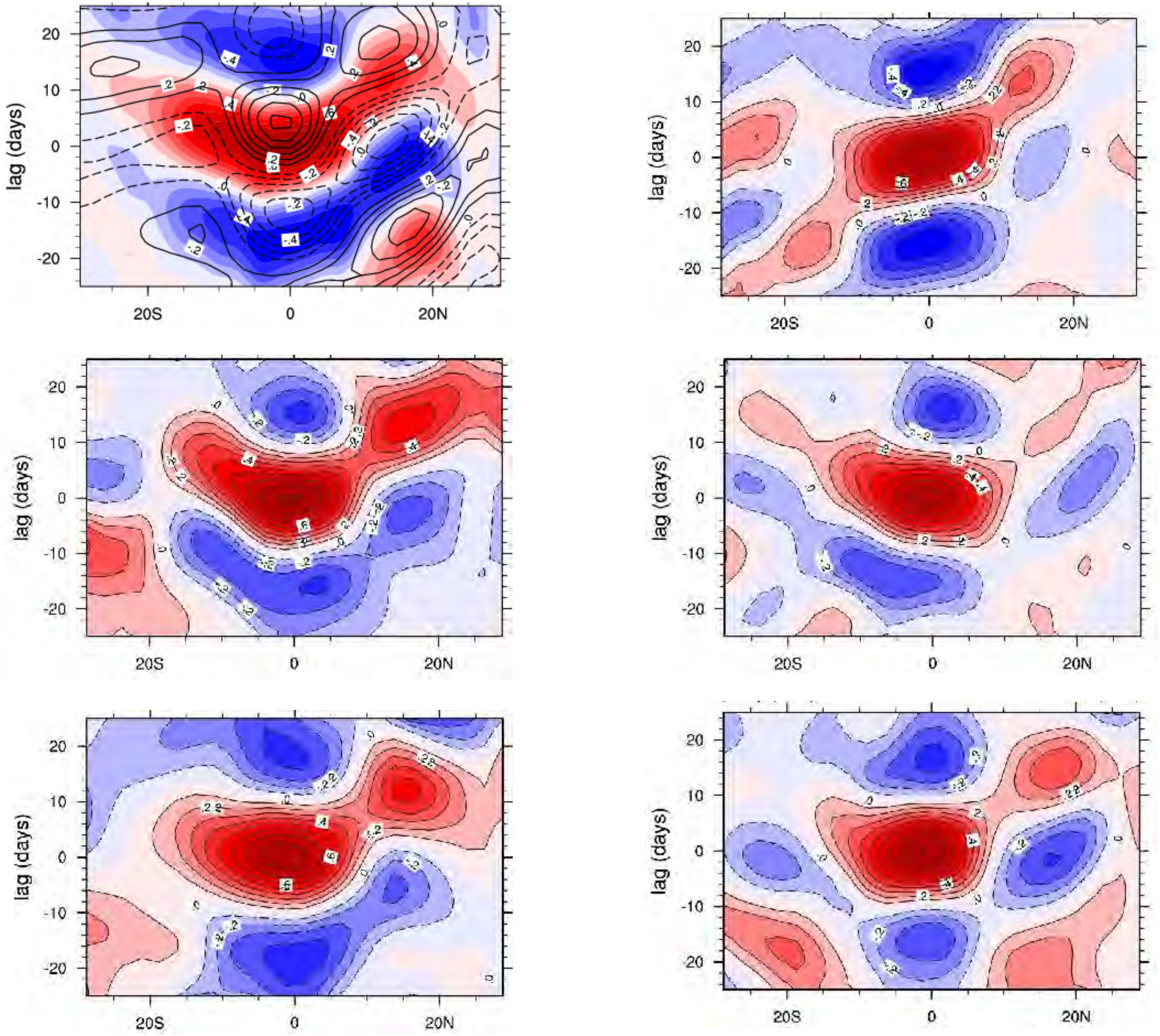

OBS

TOPO 50%

TOPO 100%

TOPO 20%

TOPO 80%

TOPO 0%

Wind shear (U200-U850)

Topo 100%

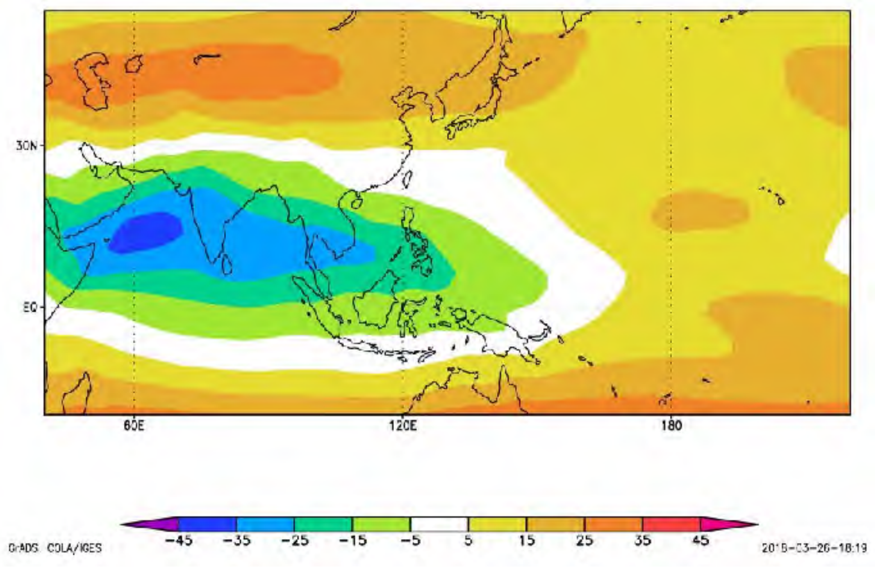

Topo 50%

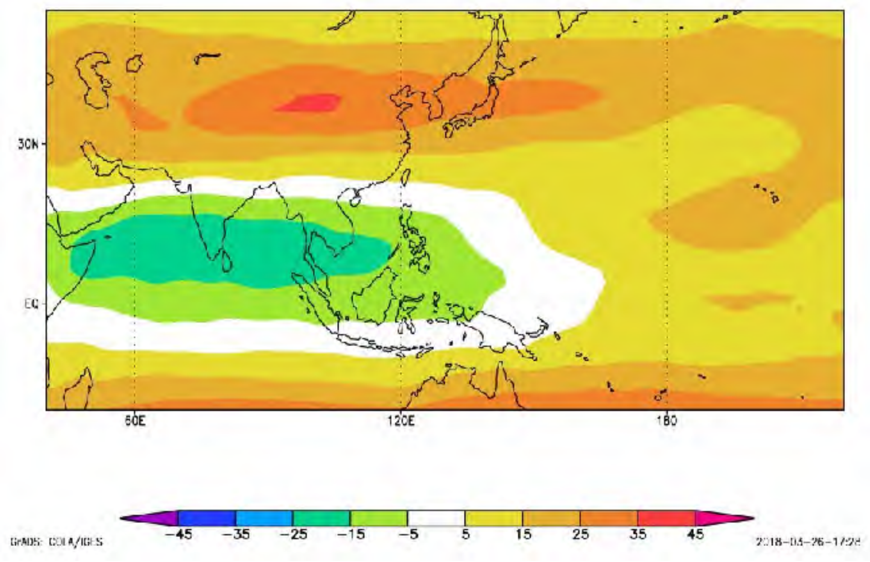

- How topography over Tibet affect northward propagation of precipitation?

Sensitivity of convective parameterization on ENSO amplitude
- role of atmospheric feedback -

Yang and Wang (2018, Submitted)

Introduction

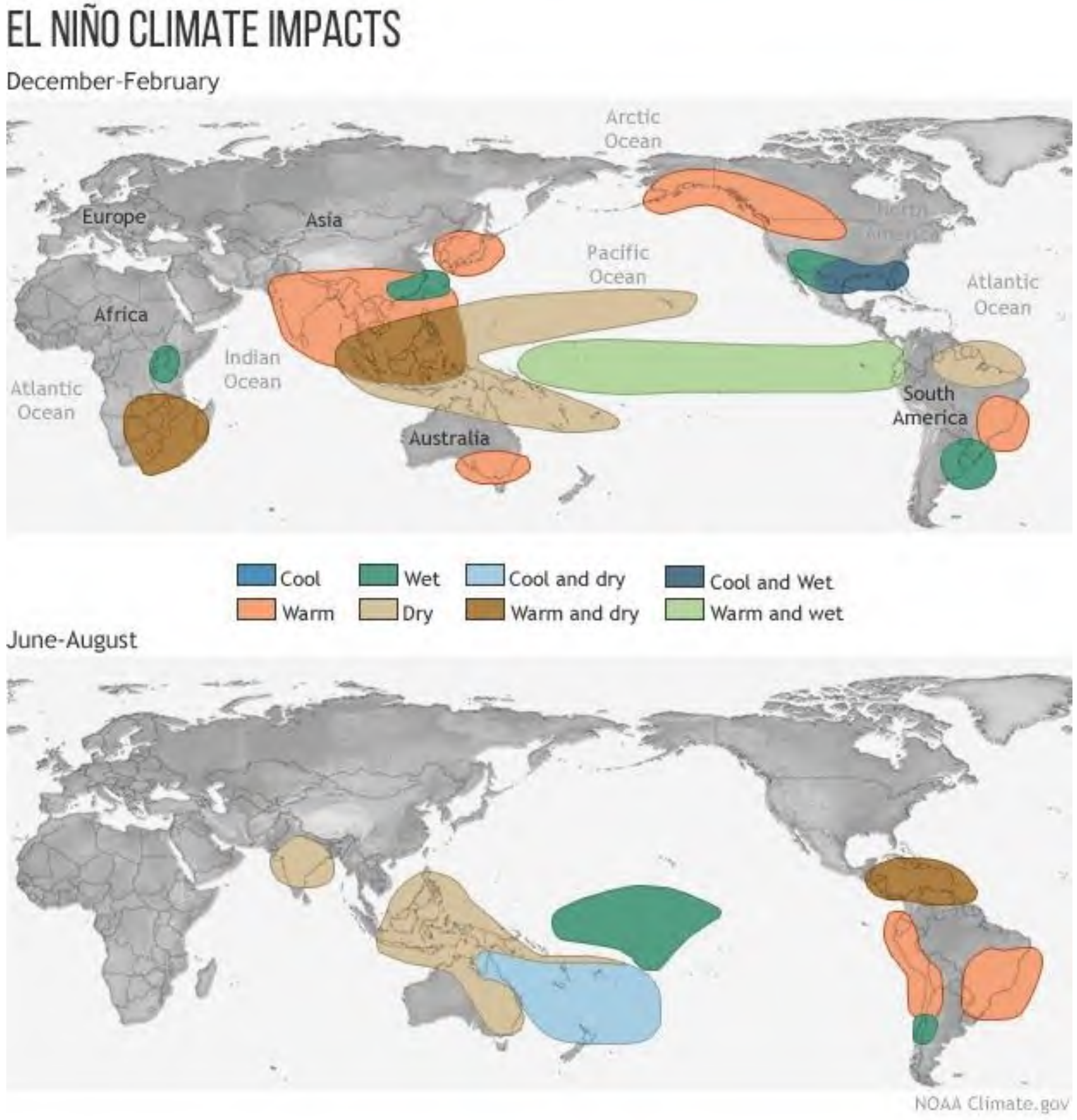

Introduction

SSTA std. dev. Nino3

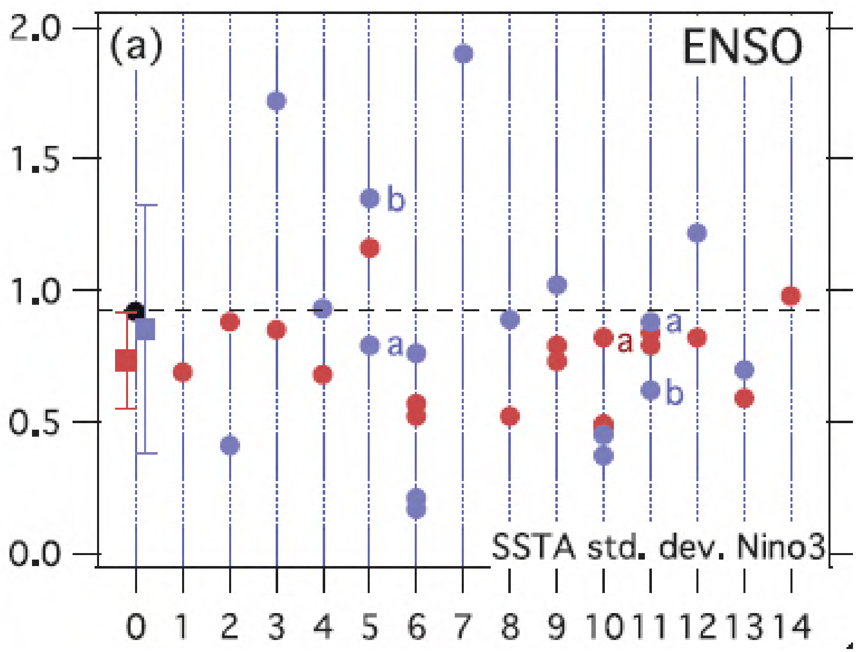

(Guilyardi et al. 2015)

Black : observation (0.9)
Blue : CMIP3, Red : CMIP5

GFDL climate model

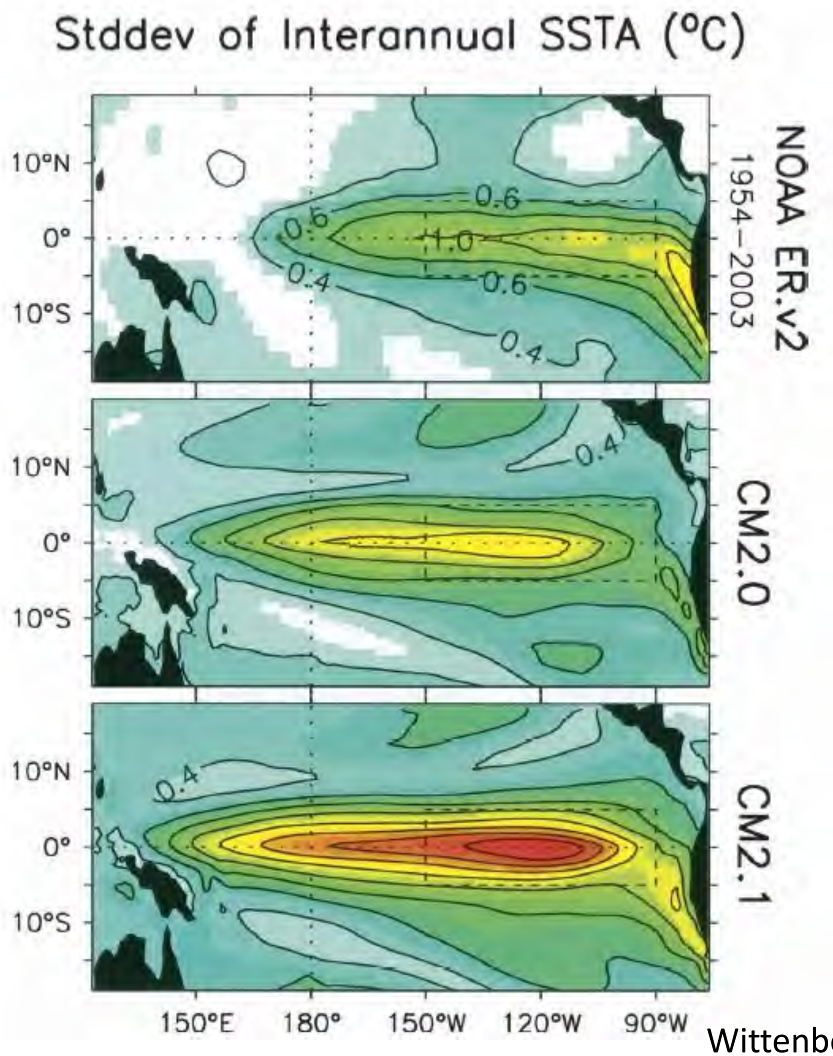

Wittenberg et al. 2006

Experiment design

Exp.	Convective parameterization	Modified scheme
CTL	Tiedtke scheme (Tiedtke, 1989)	-
TRG	Tiedtke scheme (Tiedtke, 1989)	BL depth-dependent convective trigger function
ENT	Tiedtke scheme (Tiedtke, 1989)	Increased entrainment for deep convection
CMP	Tiedtke scheme (Tiedtke, 1989)	Reduced conversion rate of cloud water to rainfall
MOD	Tiedtke scheme (Tiedtke, 1989)	TRG+ENT+CMP

- 1990’s fixed forcing
- NESMv3-SR
- 50yr integrations are used for analysis

ENSO interannual variability

OBS

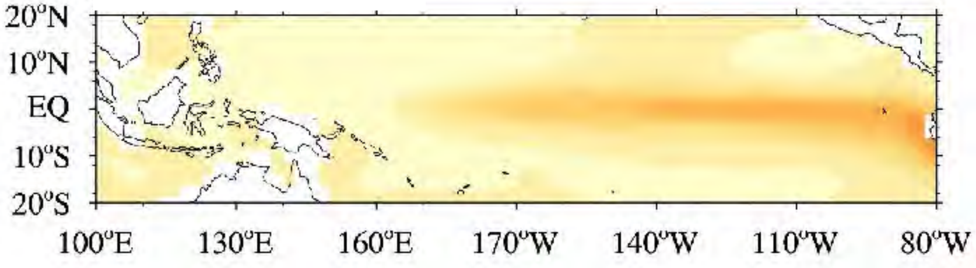

MOD

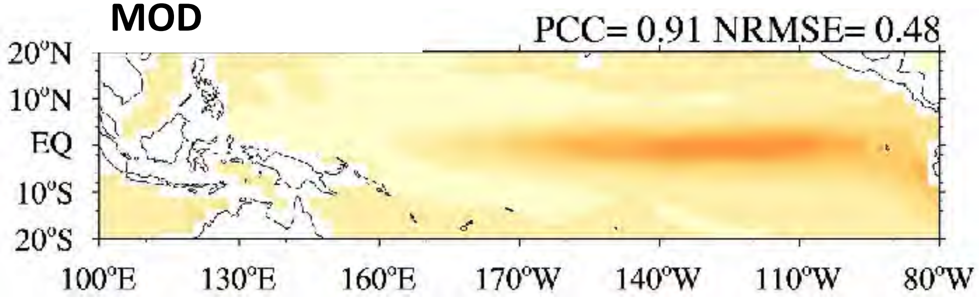

CTL

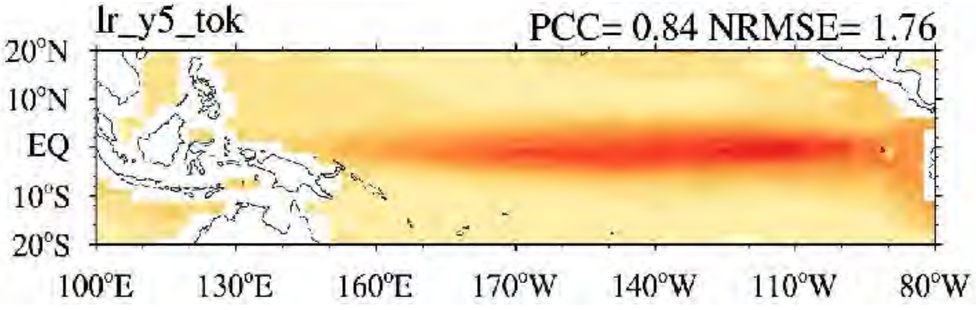

CMP

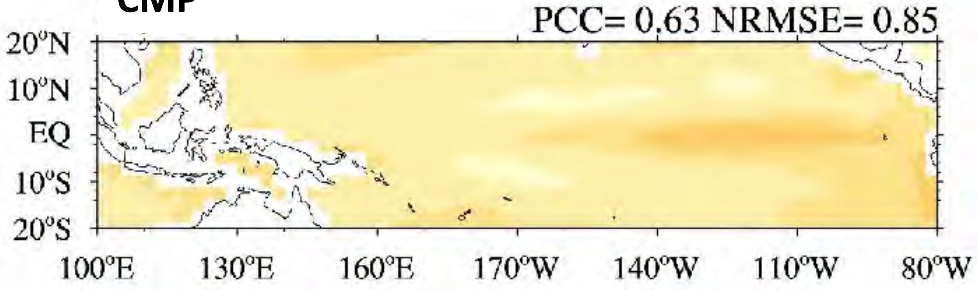

TRG

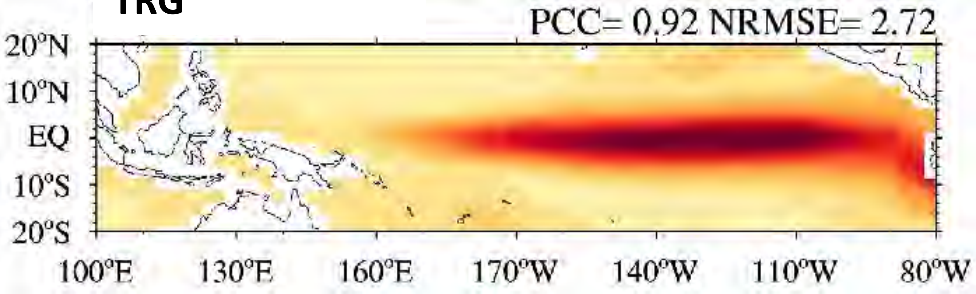

ENT

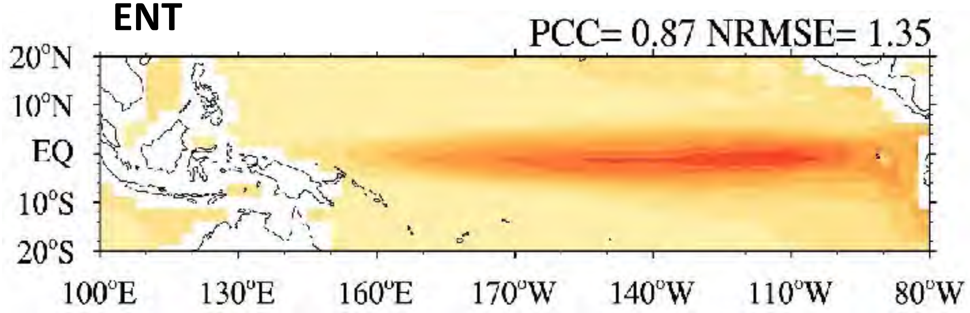

What controls SST variability? – budget analysis

$$I_{BJ} = \frac{R}{2},$$

$$R = CD + TD + ZA + EK + TC.$$

IBJ : Bjerknesindex (An et al. 1999)

CD: damping feedback by ocean curren
TD : thermodynamic damping
ZA : Zonal advective feedback
EK : Ekman feedback
TC : thermocline feedback

$$ZA = \mu_a \beta_u \left\langle \frac{-\partial \bar{T}}{\partial x} \right\rangle_E,$$

$$EK = \mu_a \beta_w \left\langle \frac{-\partial \bar{T}}{\partial z} \right\rangle_E,$$

$$TC = \mu_a \beta_h \left\langle \frac{\bar{w}}{H_1} \right\rangle_E.$$

$$CD = -\left(\frac{\langle \bar{u} \rangle_E}{L_x} + \frac{\langle -2y\bar{v} \rangle_E}{L_y^2} + \frac{\langle H(\bar{w})\bar{w} \rangle_E}{H_m} \right),$$

$$TD = -\alpha,$$

$$-\alpha = -\alpha_{SW} - \alpha_{LW} - \alpha_{SH} - \alpha_{LH},$$

Ocean budget analysis

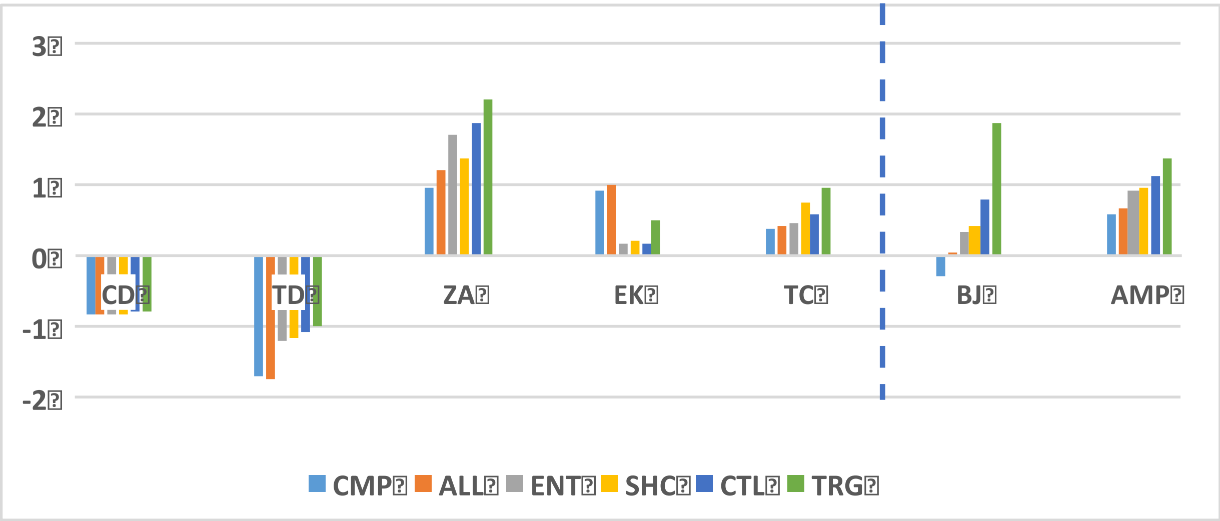

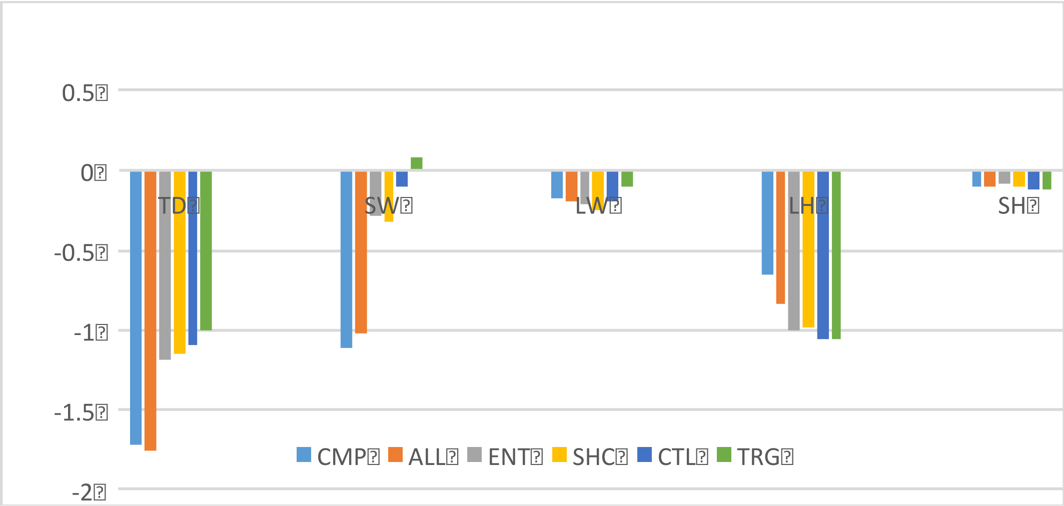

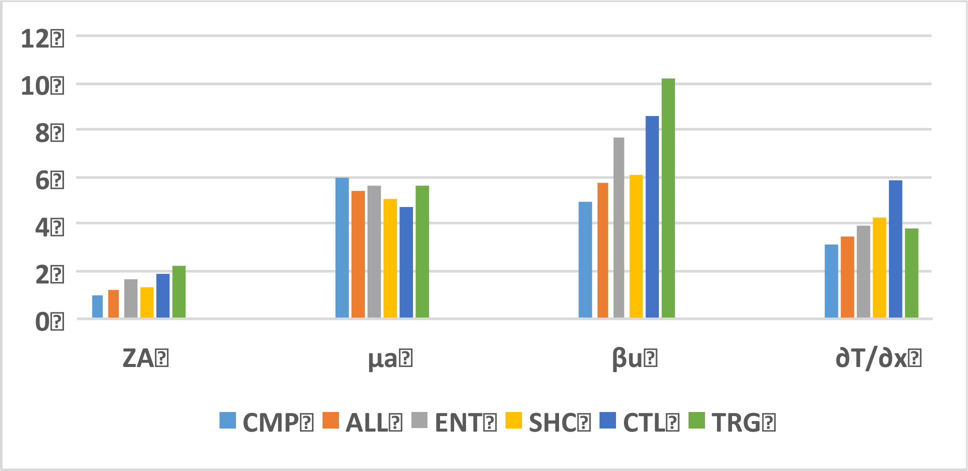

Coupled strength (Zonal wind stress feedback)

Zonal wind stress regressed on Nino3.4

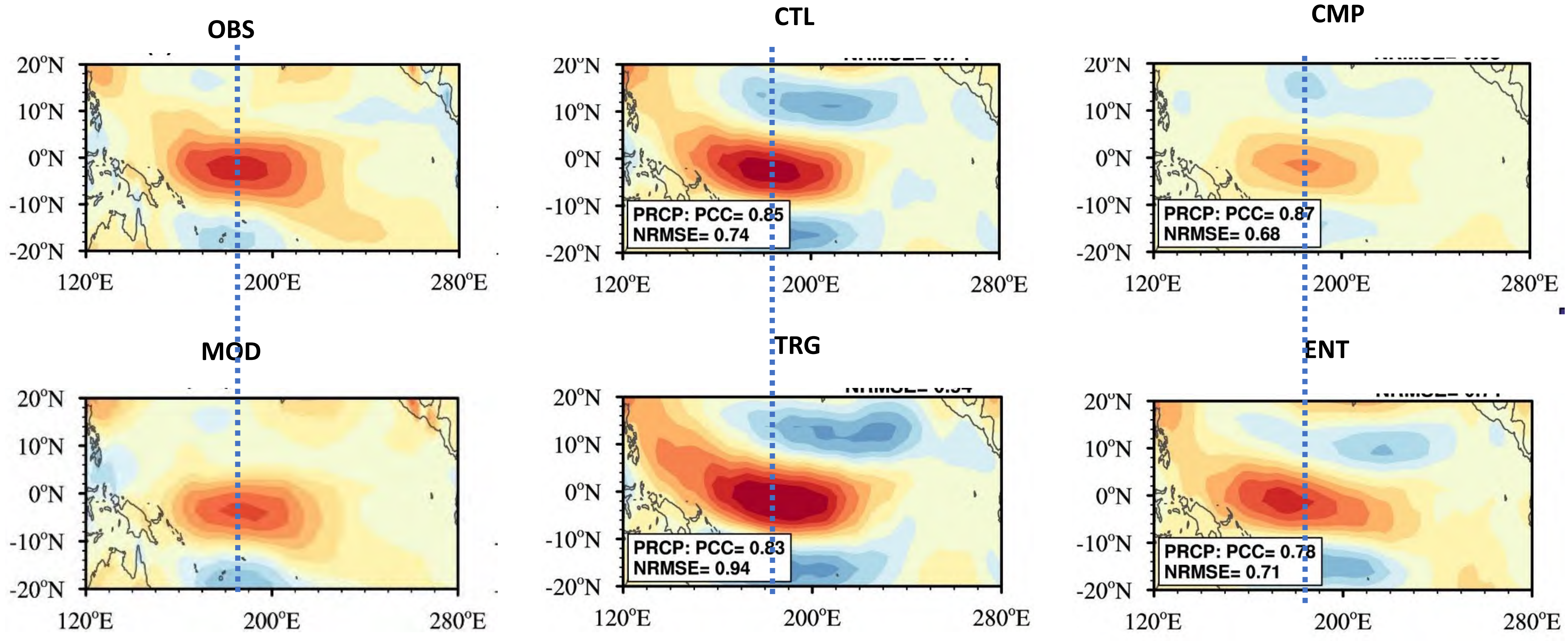

Coupled strength (Zonal wind stress feedback)

Precipitation regressed on Nino3.4

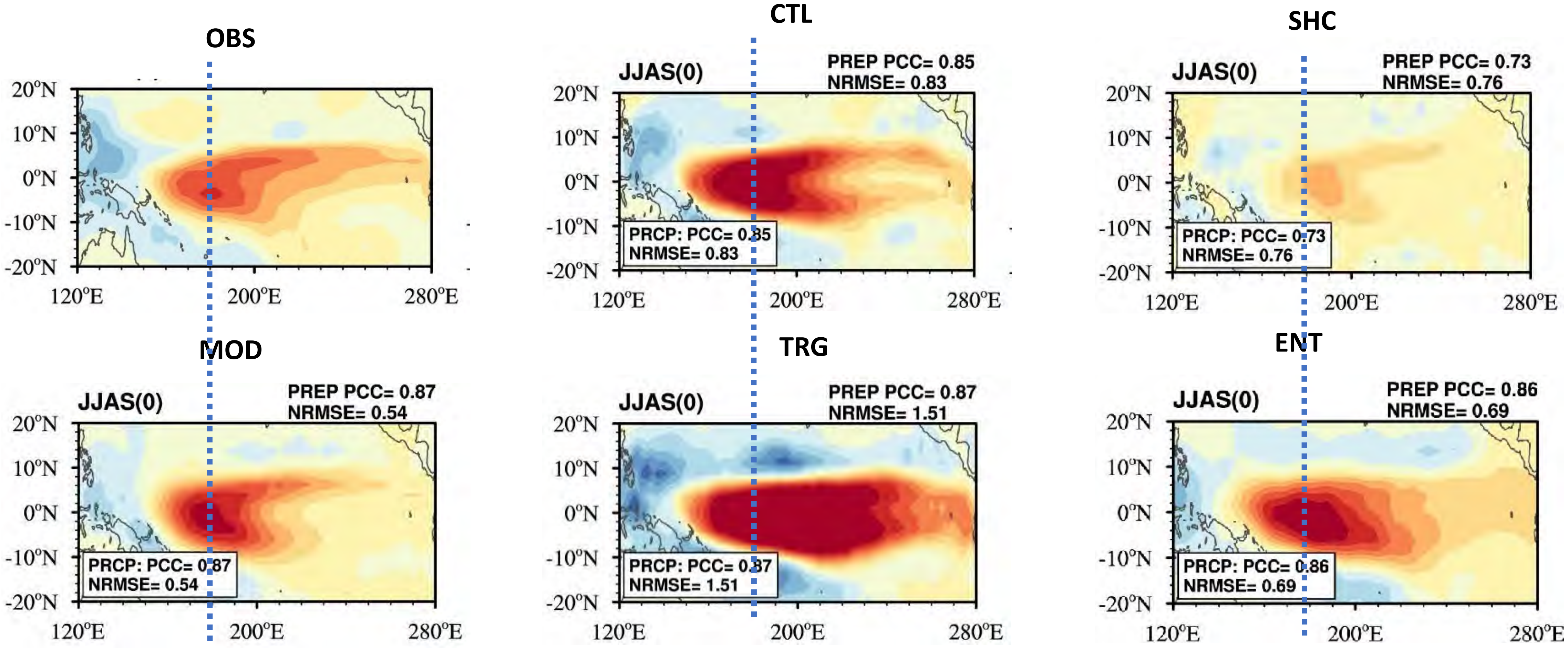

Summary

1. ENSO variability is sensitive to atmospheric convective parameterizations

2. The advective and thermodynamics feed is critical for ENSO amplitude

3. The advective feedback depends on change of wind stress, which results from change of precipitation.

4. Change of cloud by modified parameterization affect thermodynamic feedback

“Sensitivity of convective parameterization on East Asia monsoon ”
-”

Limitation of climate model simulation

Summer mean precipitation

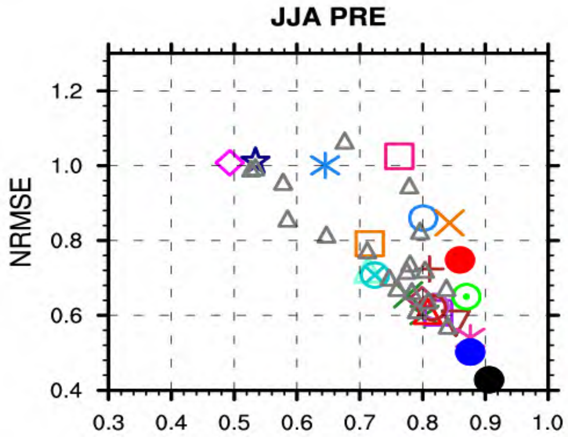

Seasonal evolution

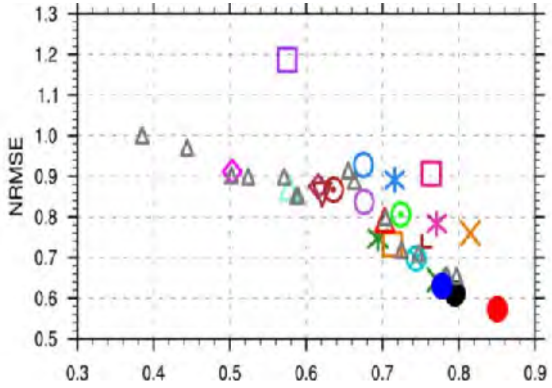

EASM-ENSO relationship

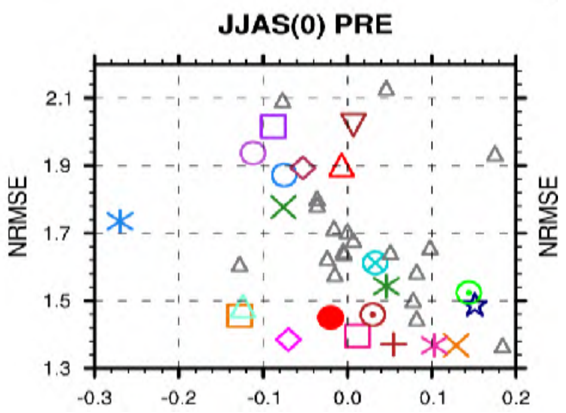

Multi EOF (PR&GH850)

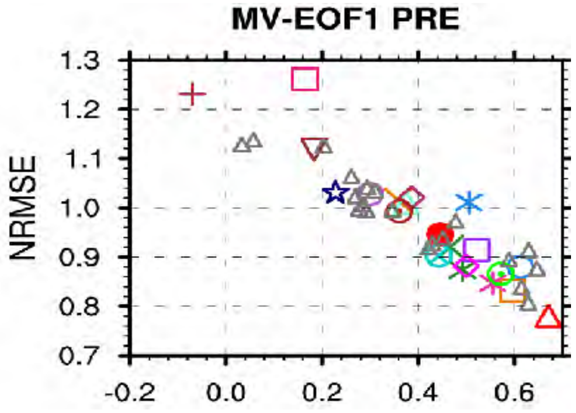

Model problems – Large-scale circulation

OBS

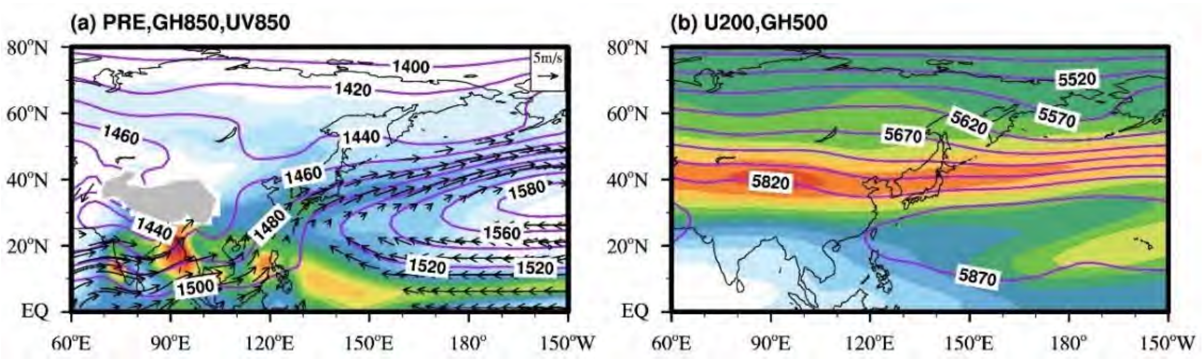

NUIST_CTL

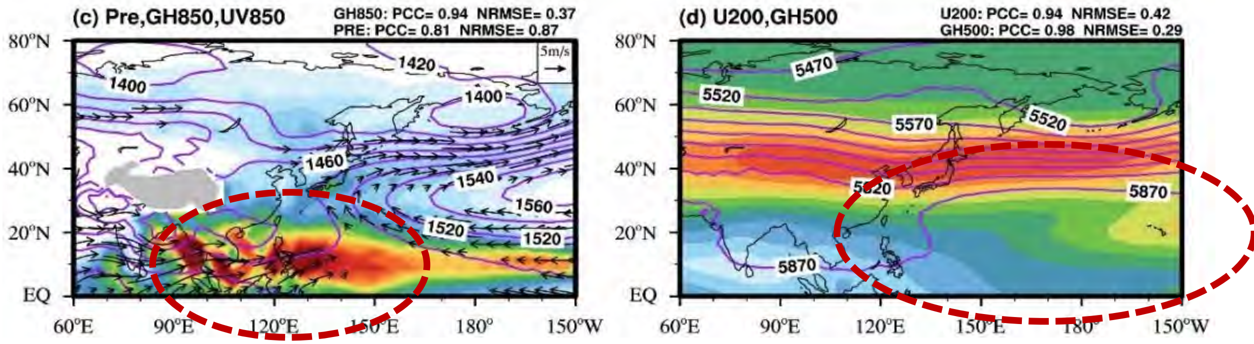

- WPSH : north & westward shift
- Excessive precipitation over WP

Model problems – Monsoon onset

SCS Index (5°–15°N and 110°–120°E)
(Wang et al, 2004)

OBS

SST

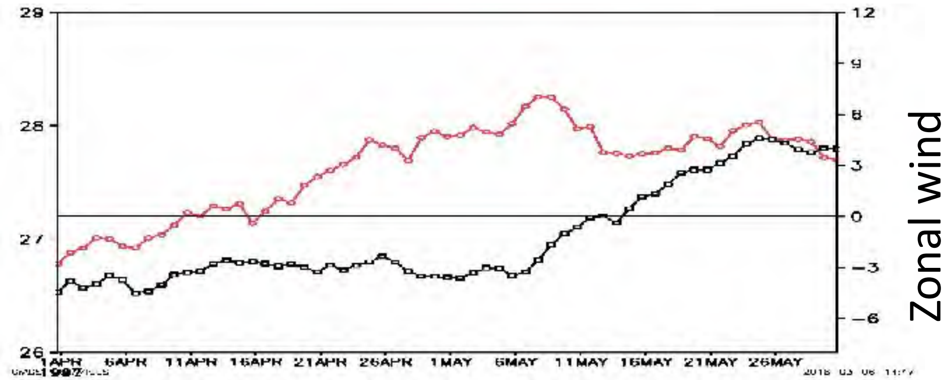

Zonal wind

NUIST_CTL

SST

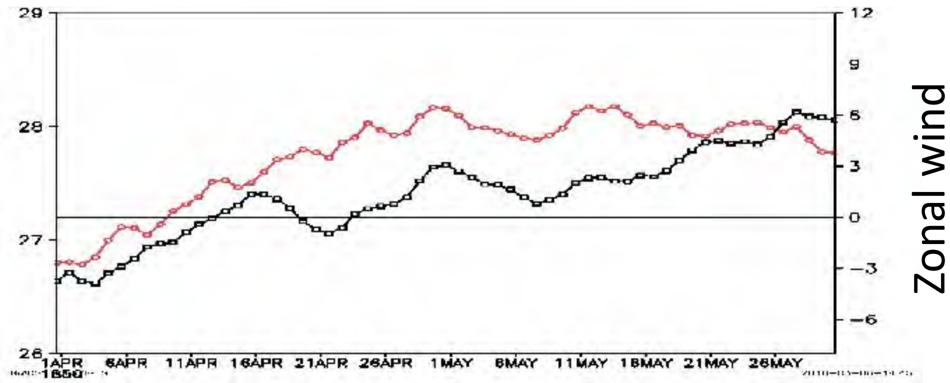

Zonal wind

SST

Zonal wind

- Delayed response of convection on increased SST
- Too sensitive to change of SST

Model problems : EAWM-ENSO relationship

Correlation of rainfall & NINO3.4

OBS

NUIST_CTL

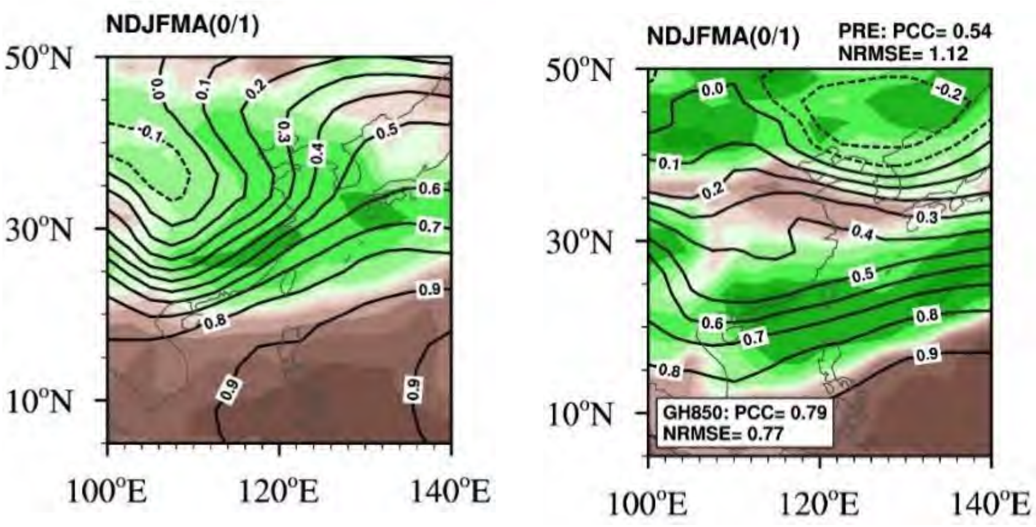

Interannual variability

OBS

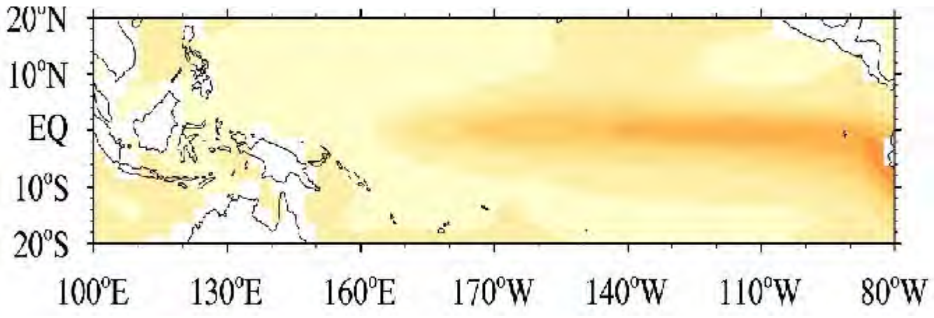

NUIST

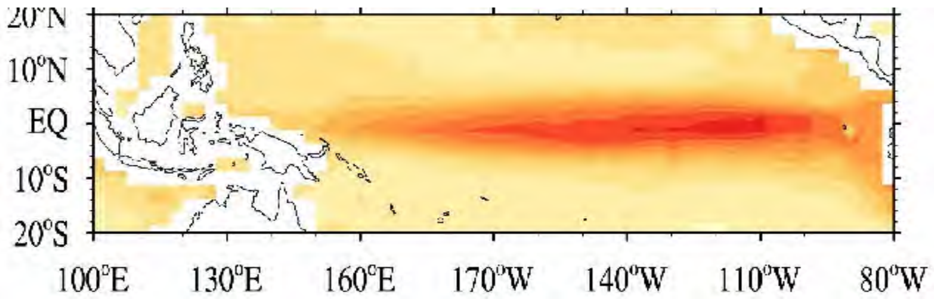

- Poor horizontal pattern
- Too strong response to ENSO

- Strong SST variability
- Shift to westard

Observed features

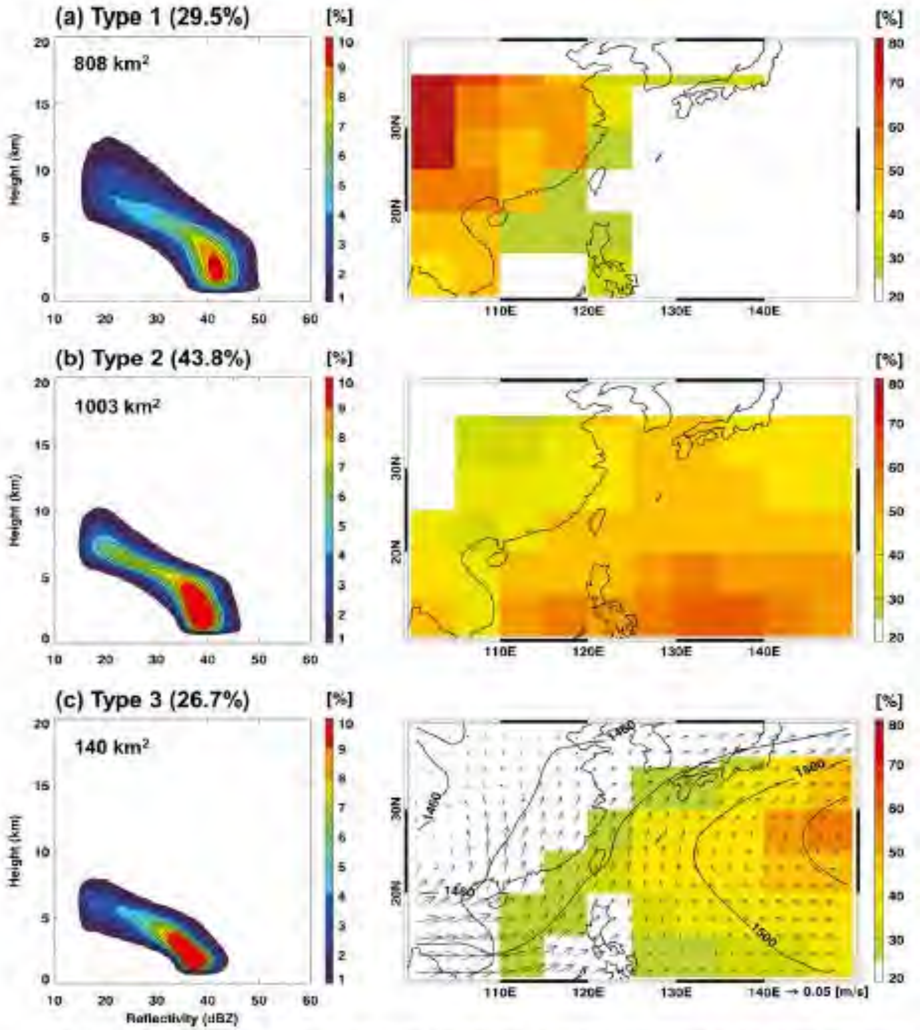

FIG. 1. (a)–(c) (left) Vertical structure and (right) occurrence frequency distribution of the heavy rain types classified by *K*-means clustering analysis. The percentage in the (left) represents the percentage occurrence of the corresponding type. While the area given in the (left) represents the rain area of a $5° \times 5°$ grid box, but averaged over the entire domain. Geopotential height (gpm, solid lines) and water vapor flux (m s^{-1}, arrows) for the 10-yr summer mean at 850-hPa level are also shown in the bottom-right figure.

- Land : deep clouds
- Ocean ; middle or shallow clouds

Enhancing shallow convection

Experiment design

Exp.	Convective parameterization	Modified scheme
CTL	Tiedtke scheme (Tiedtke, 1989)	-
TRG	Tiedtke scheme (Tiedtke, 1989)	BL depth-dependent convective trigger function
ENT	Tiedtke scheme (Tiedtke, 1989)	Increased entrainment for deep convection
CMP	Tiedtke scheme (Tiedtke, 1989)	Reduced conversion rate of cloud water to rainfall
MOD	Tiedtke scheme (Tiedtke, 1989)	TRG+ENT+CMP

- 1990's fixed forcing
- NESMv3-SR
- 50yr integrations are used for analysis

Large-scale climatological circulation

OBS

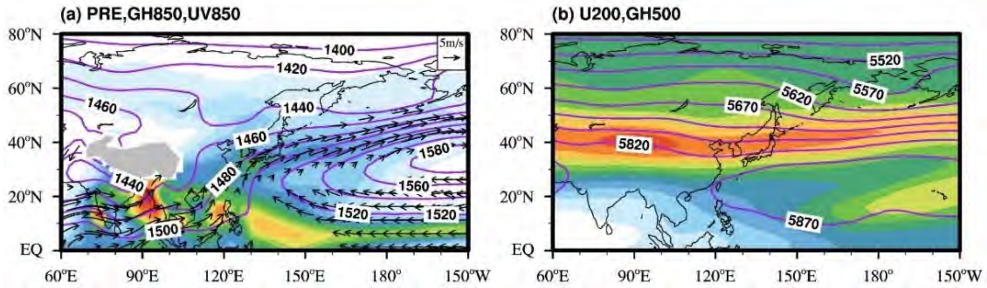

CTL

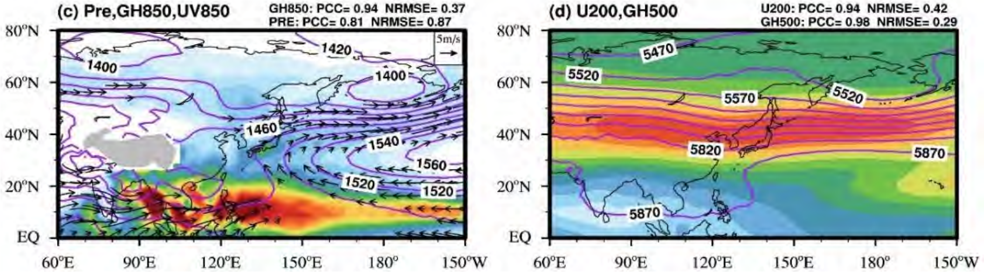

SHC

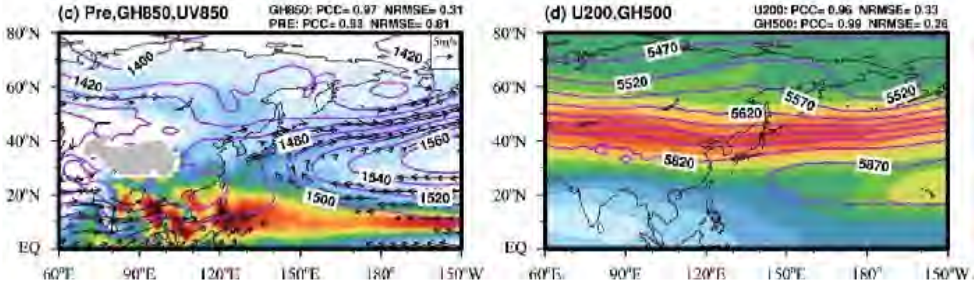

TRG

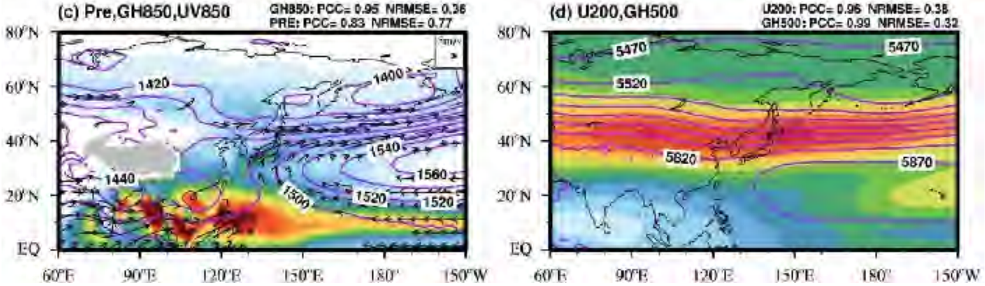

ENT

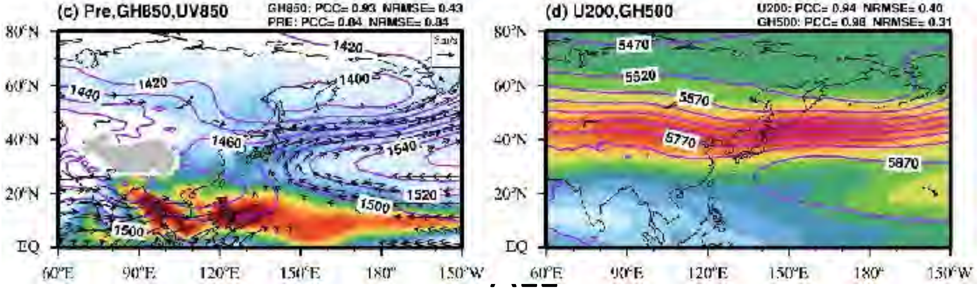

CMP

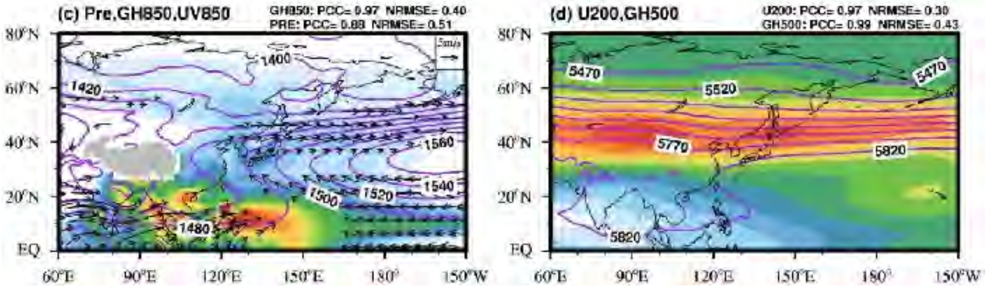

ALL

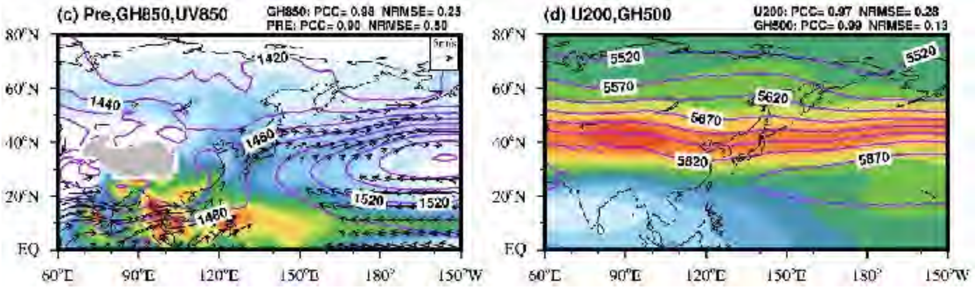

Ratio of convective to total rainfall

TRMM (Song and Smith 2008)

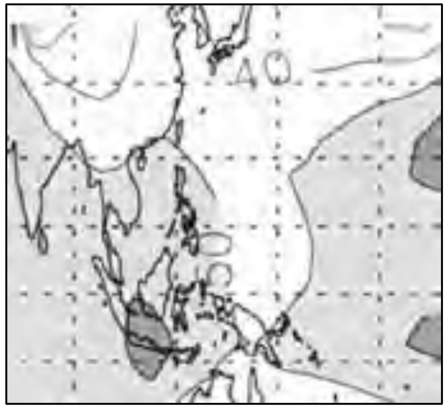

40~50%

TRG

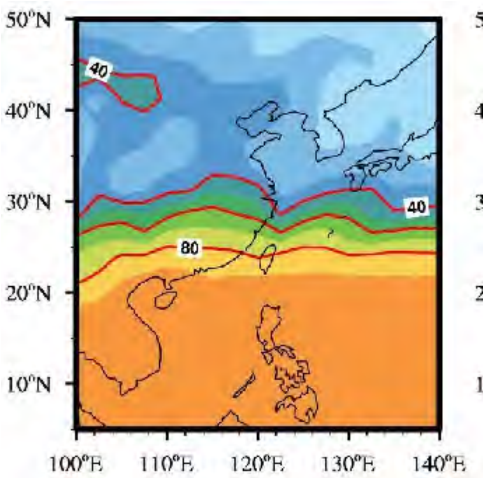

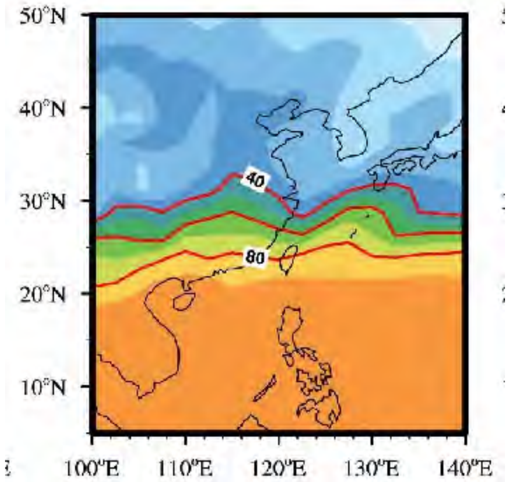

CMP

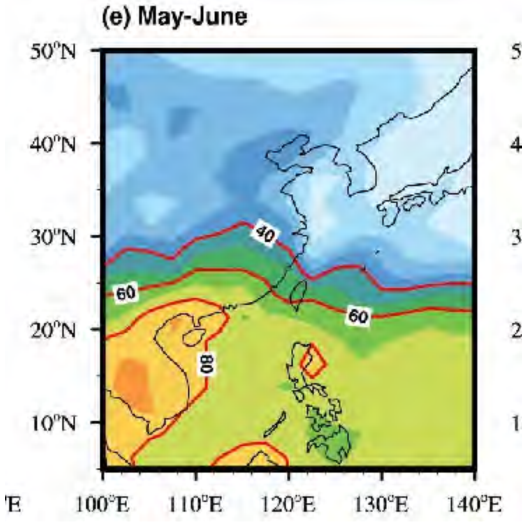

SHC

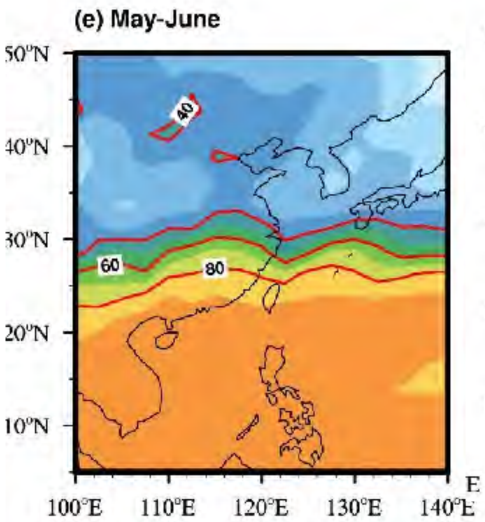

ENT

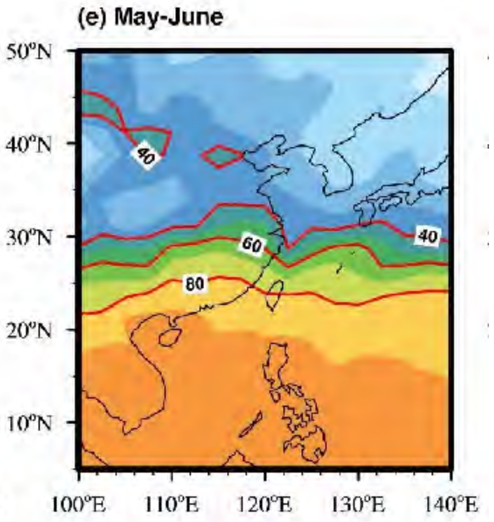

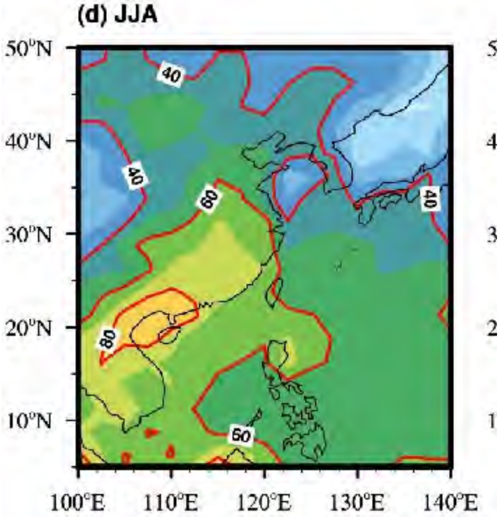

Large-scale climatological circulation

Precipitation (JJA)

Stream function & non-divergent wind (850hPa)

TRG-CTL

CMP-CTL

SHC-CTL

ENT-CTL

ALL-CTL

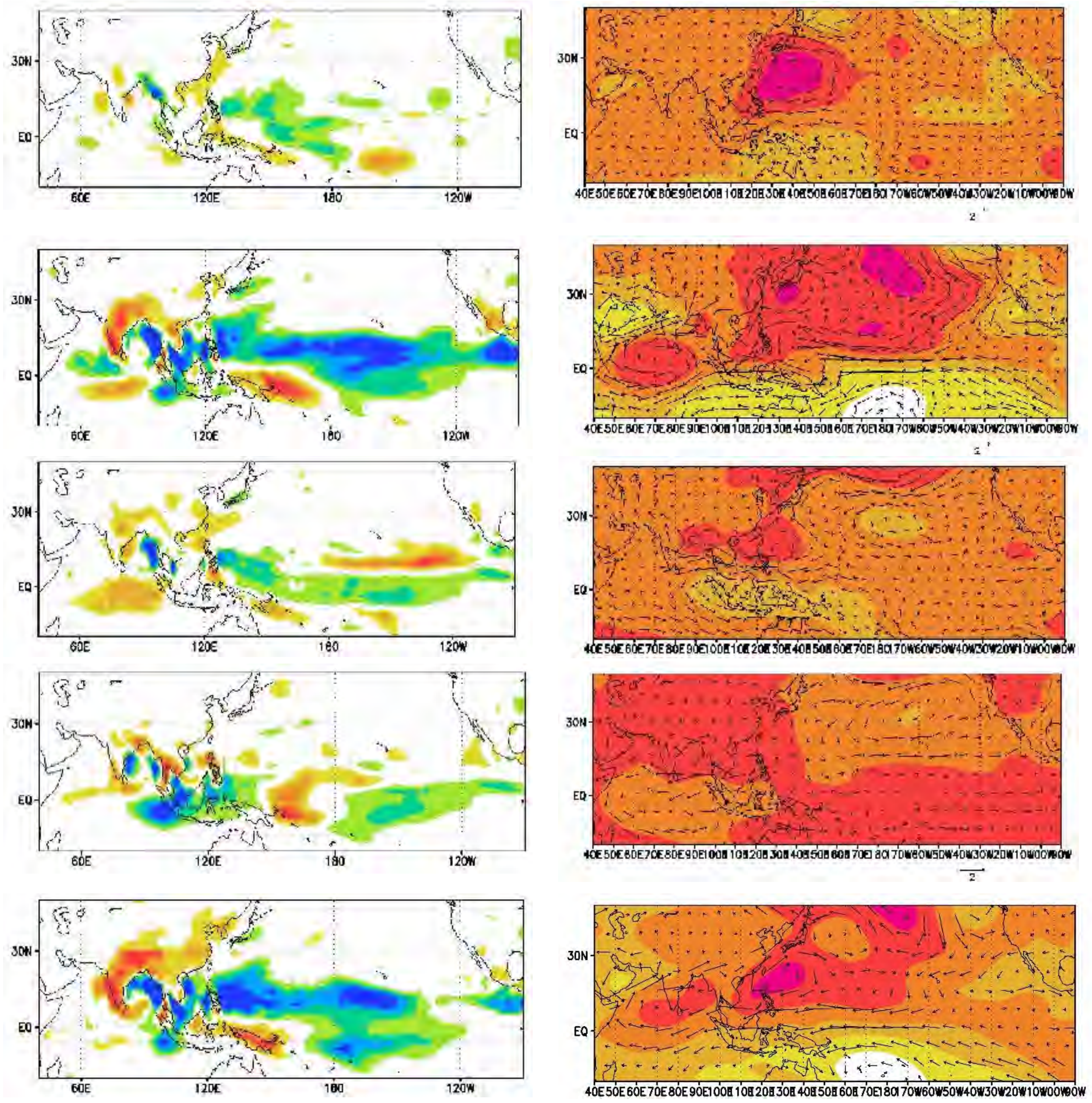

Monsoon onset

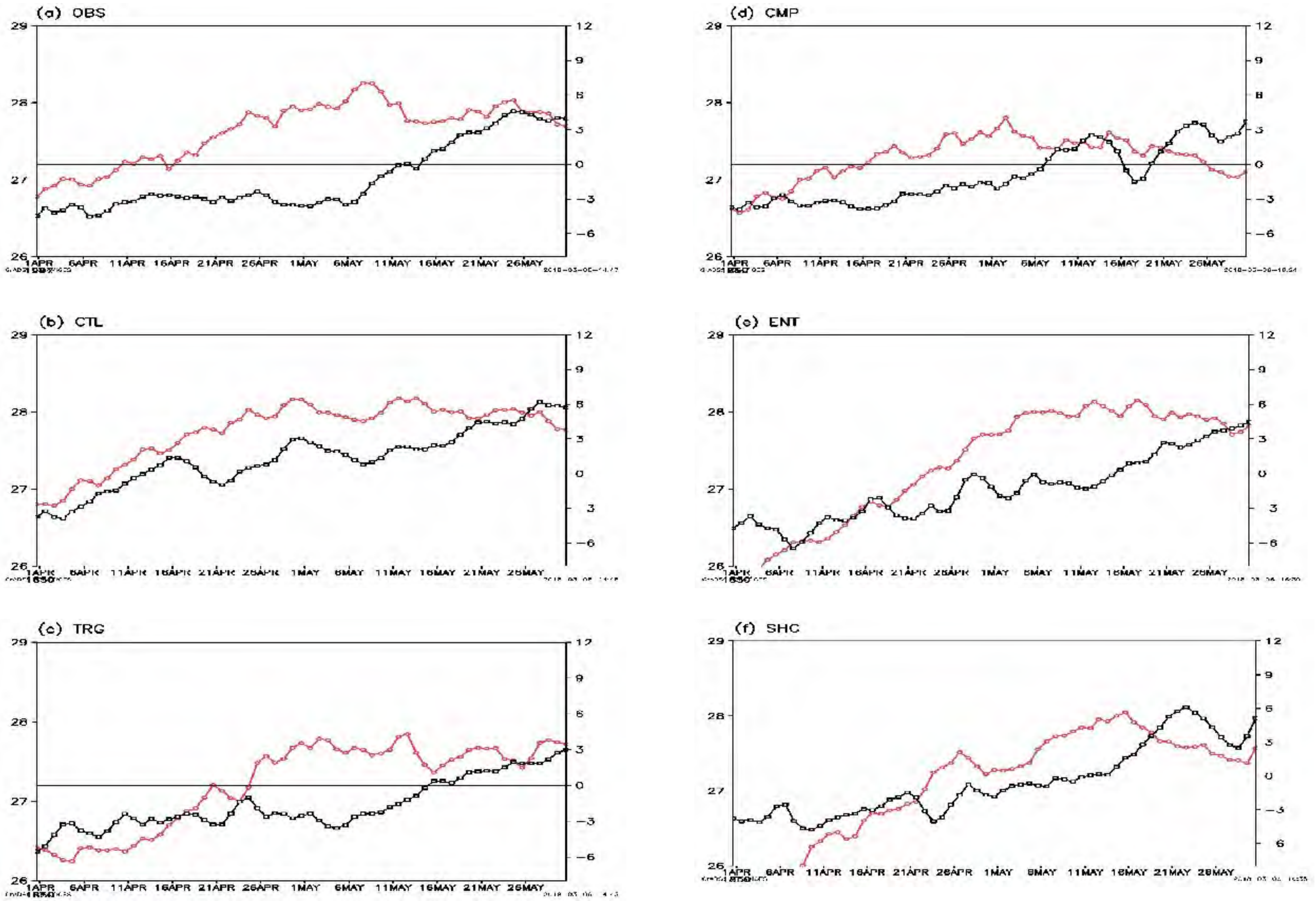

EASM-ENSO relationship

OBS

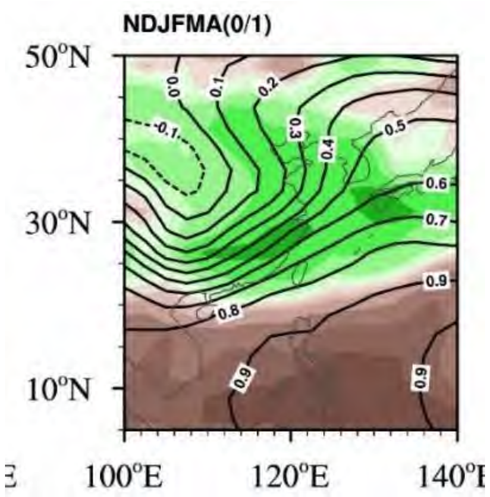

CTL

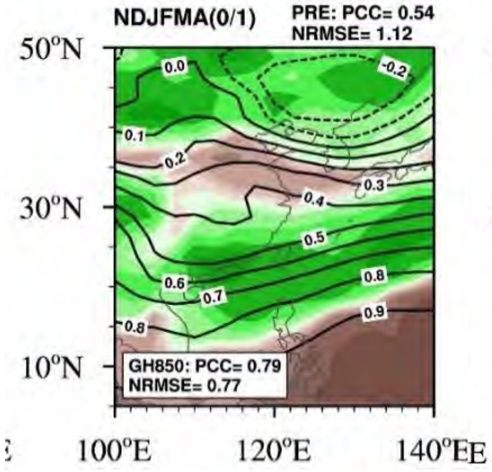

TRG

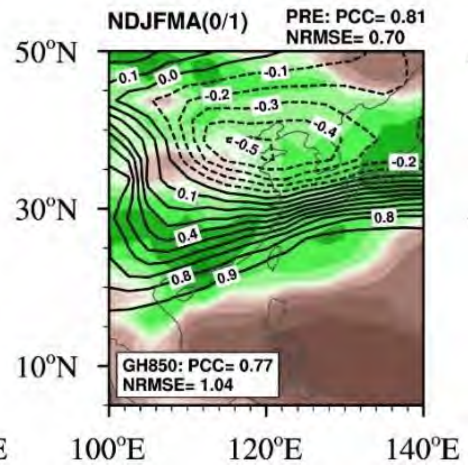

CMP

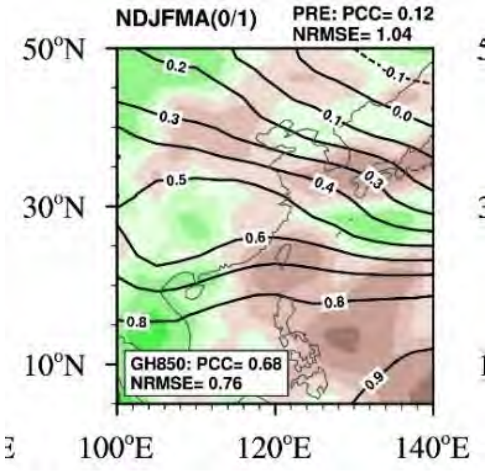

SHC

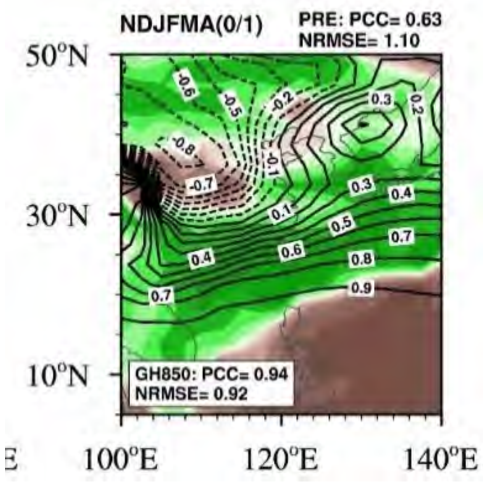

ENTR

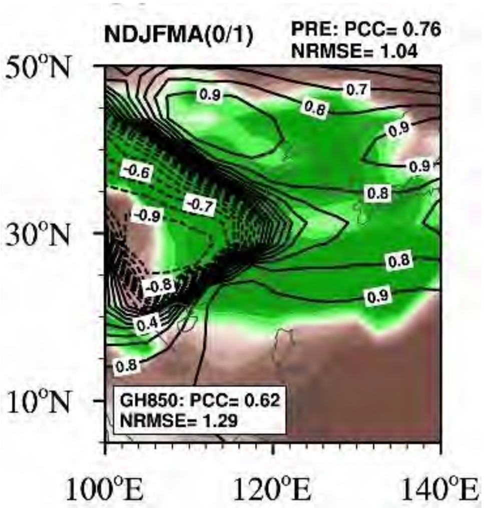

MOD

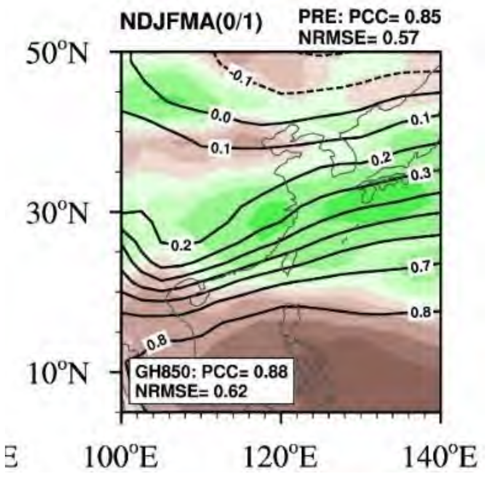

Teleconnection (regression of rainfall on wind shear index

WSI= U850 (110^{o}E -140^{o}E; 22.5^o N-32.5^{o}N) - U850 (90^{o}E -130^{o}E; 5^o N-15^{o}N)

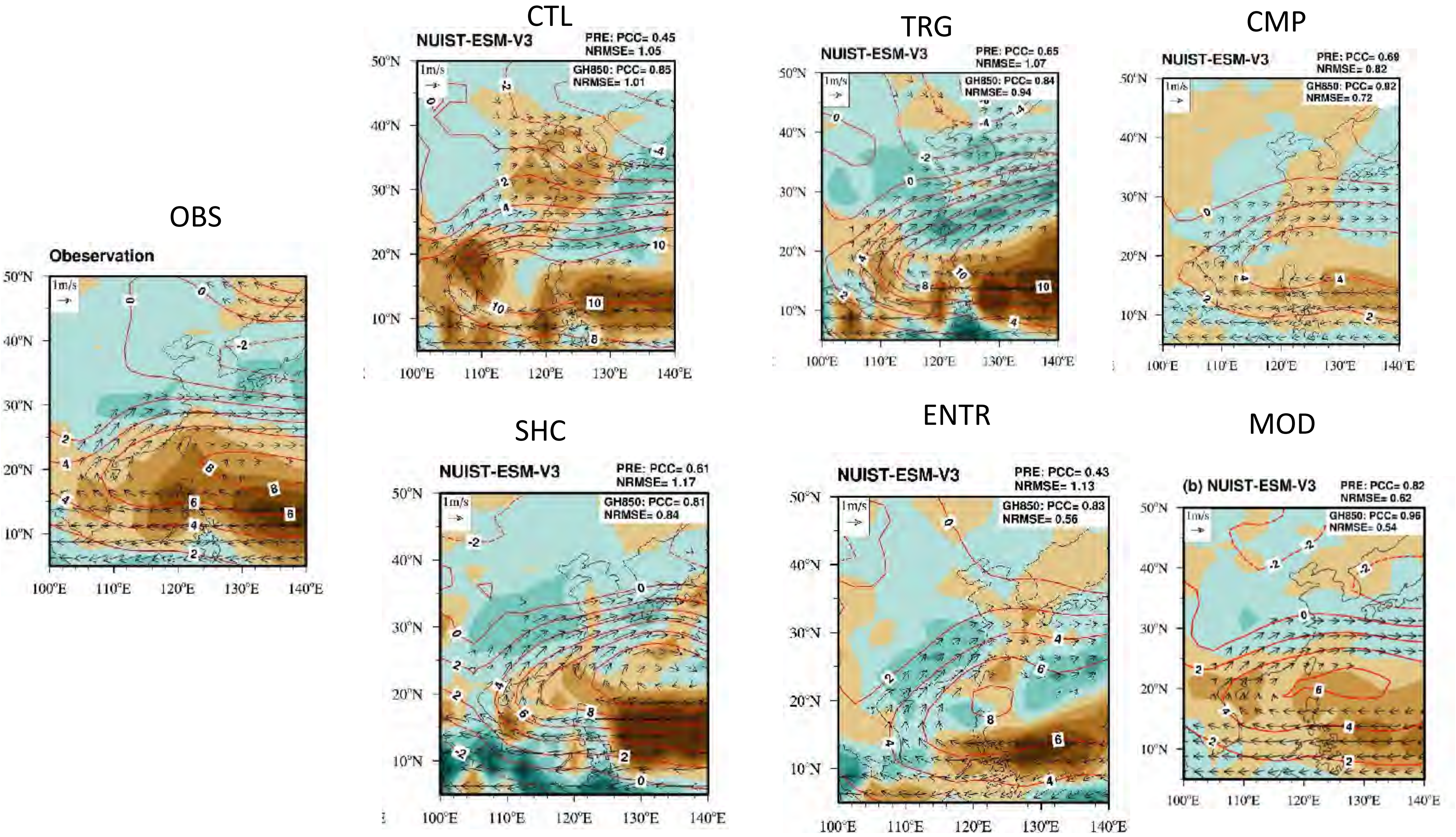

How convective parameterization affect global warming slowdown? role of atmosphere heating and circulation”

Global warming slowdown – "Hiatus"

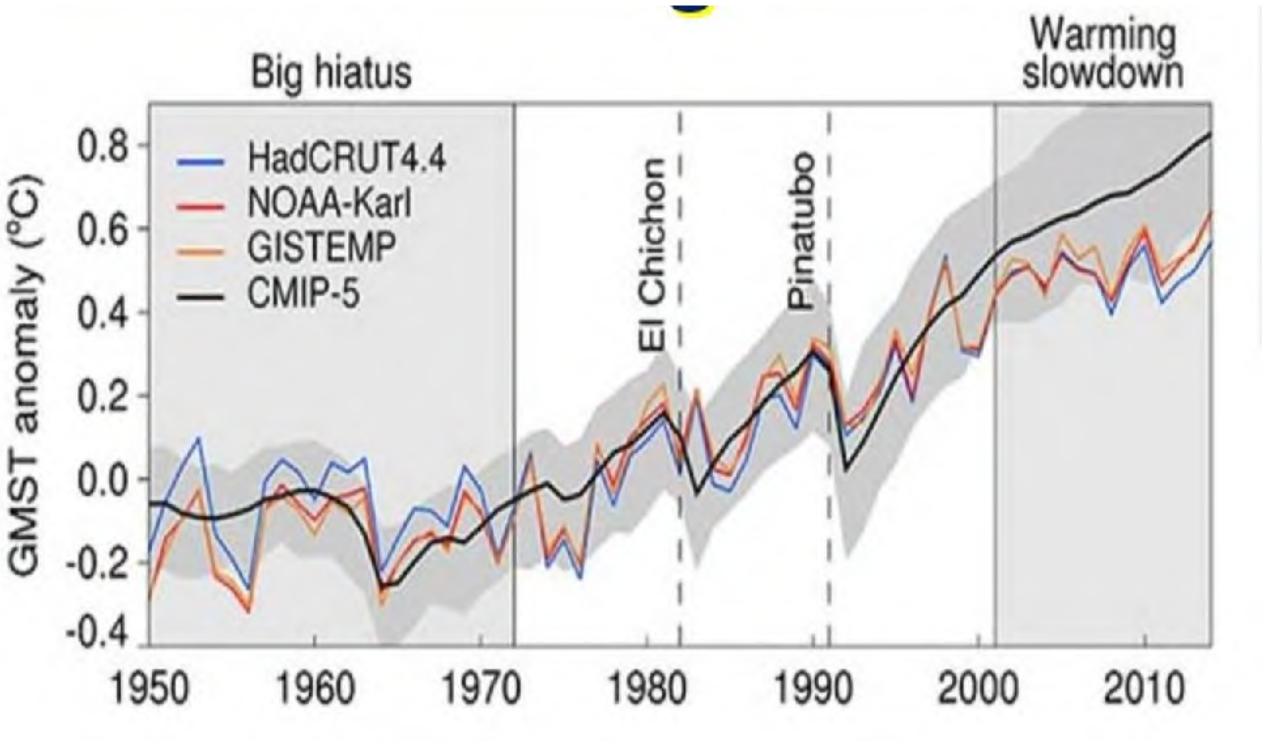

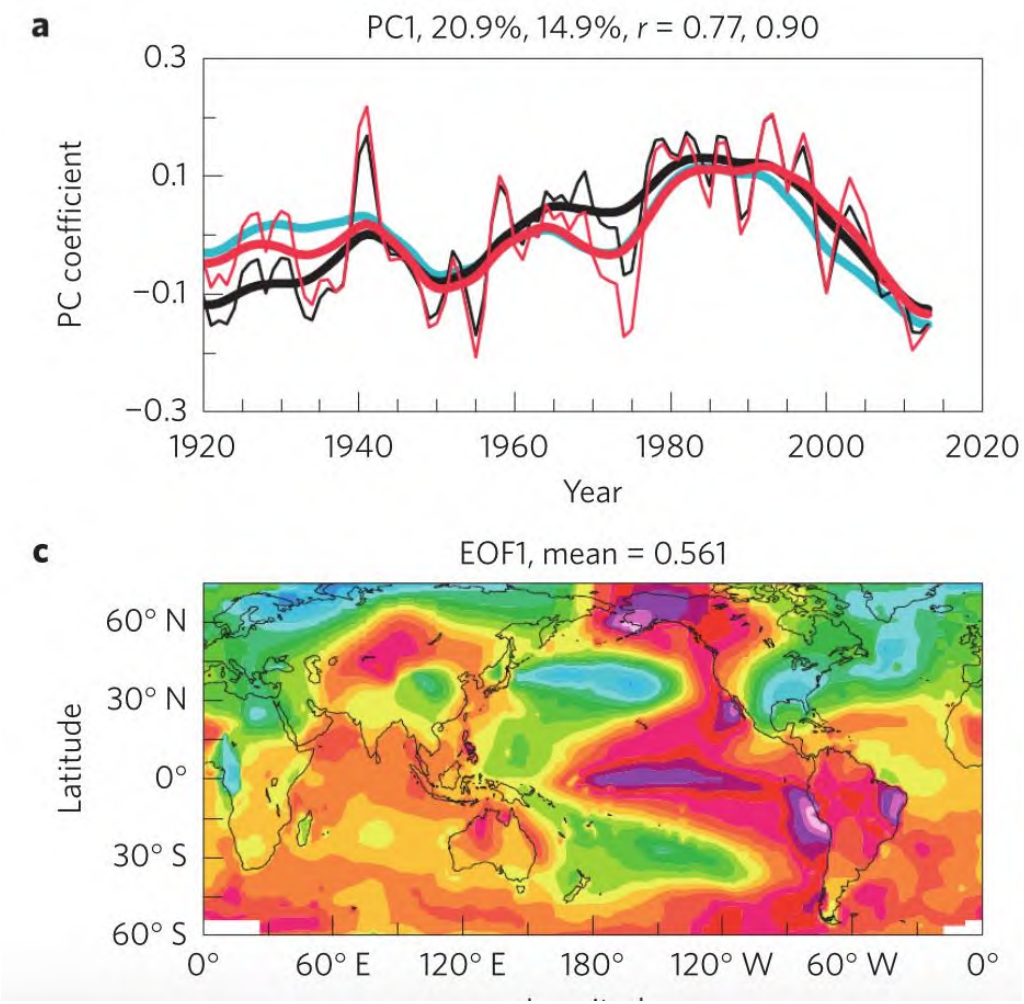

- Global warming trends after 2000yr
- OBS : slowdown
- CMIPT5: continuously warming.

Dai et al. 2015

Simulation of global warming slowdown

τ EOF1 reanalysis

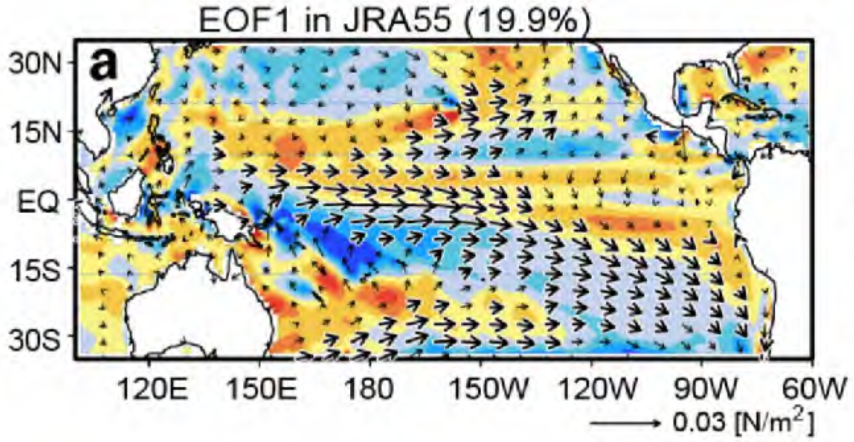

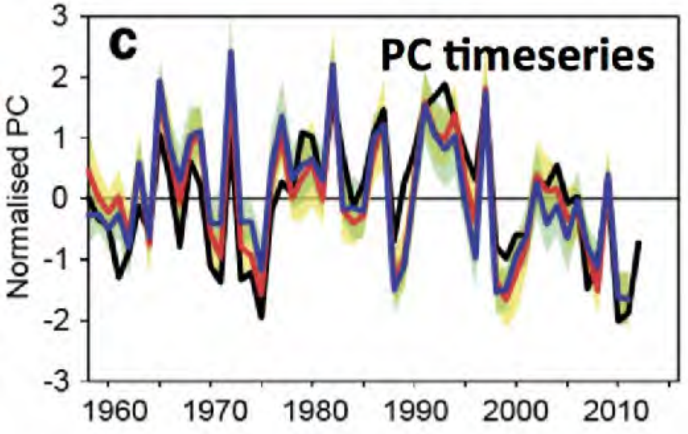

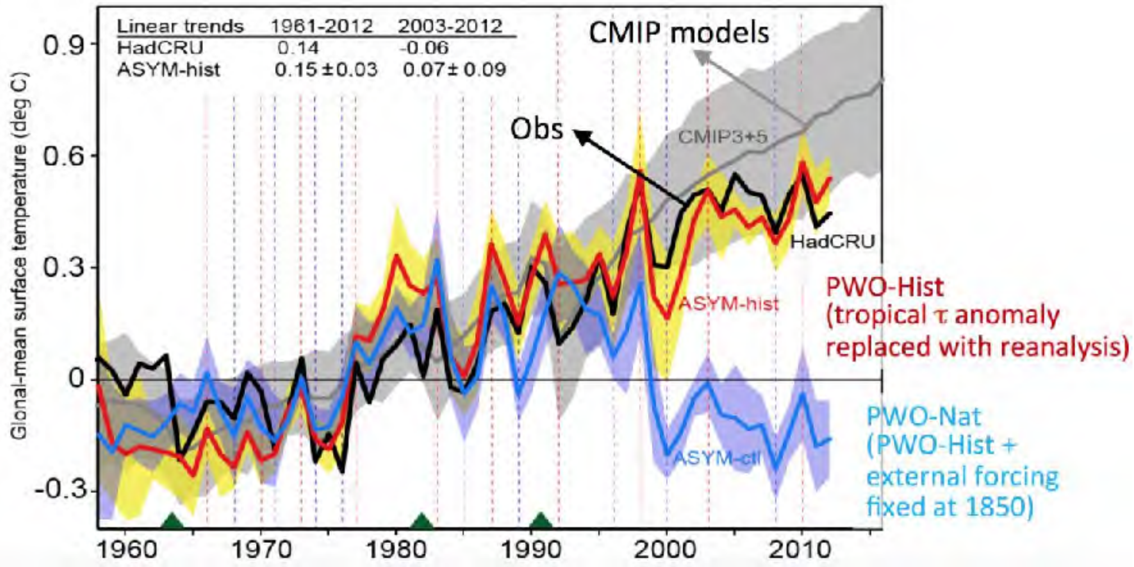

Tropical wind stress forced run
=> successful reproduction

Historical run

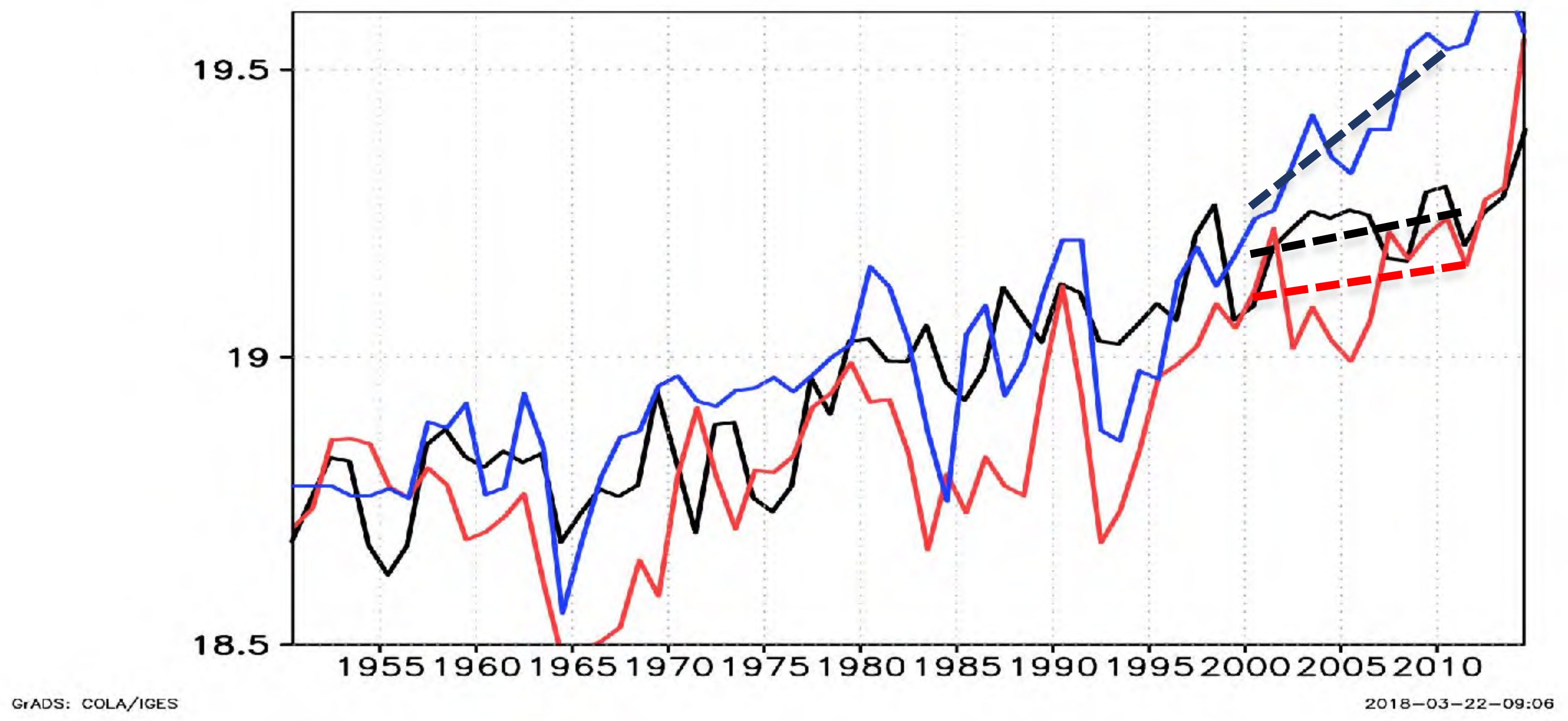

Modified convective parameterization

Original convective parameterization

Observation

Interdecadal Pacific Oscillation

OBS

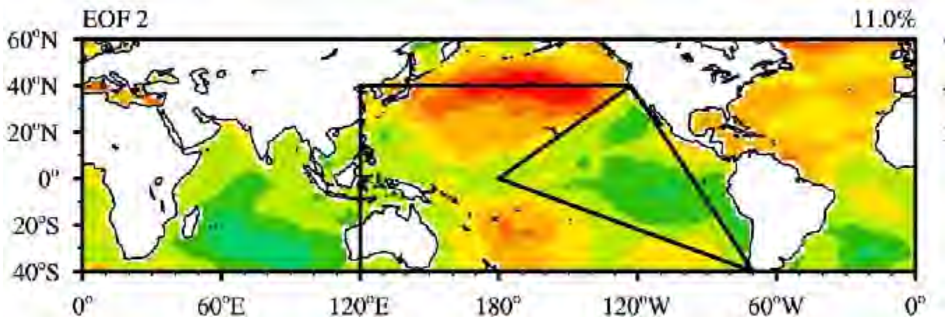

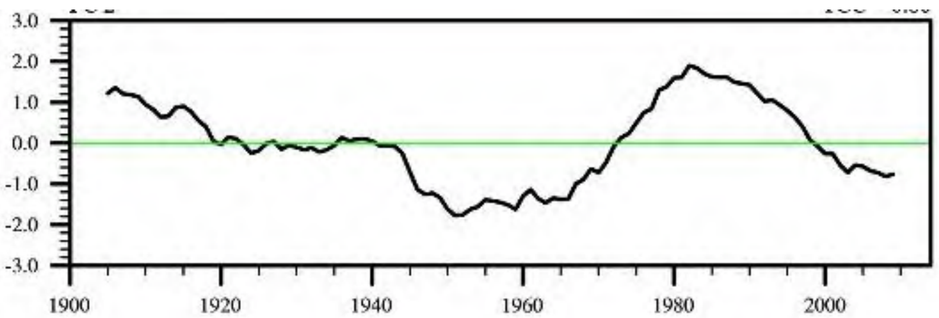

MOD

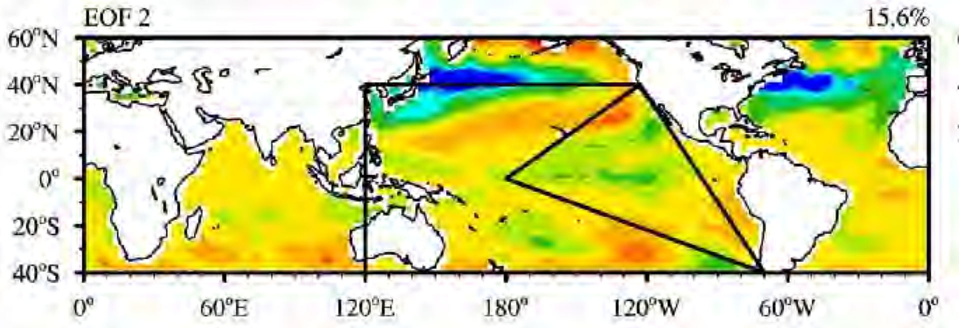

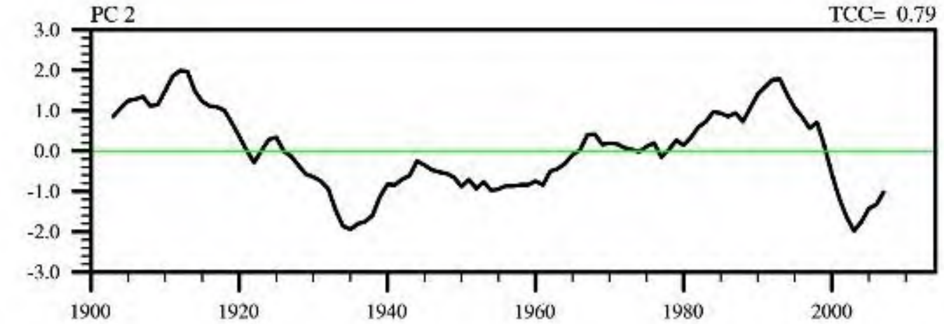

CTL

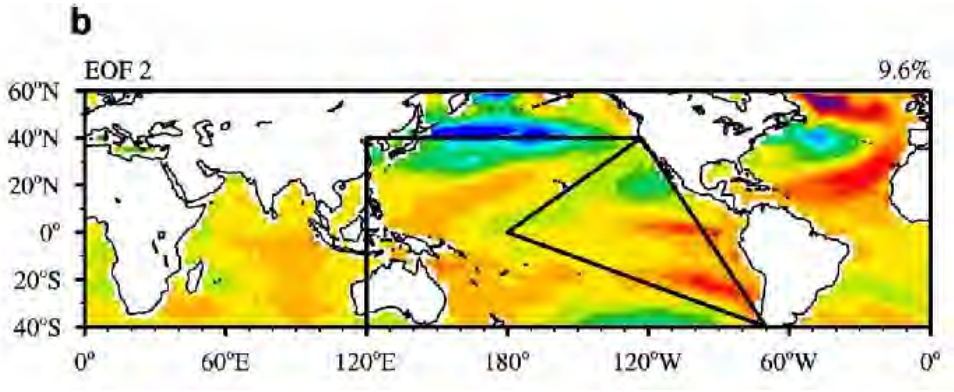

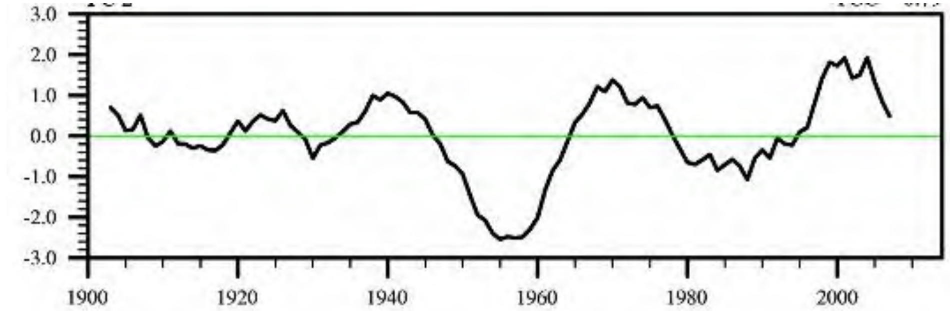

Inter-Decadal oscillation of zonal wind stress

OBS

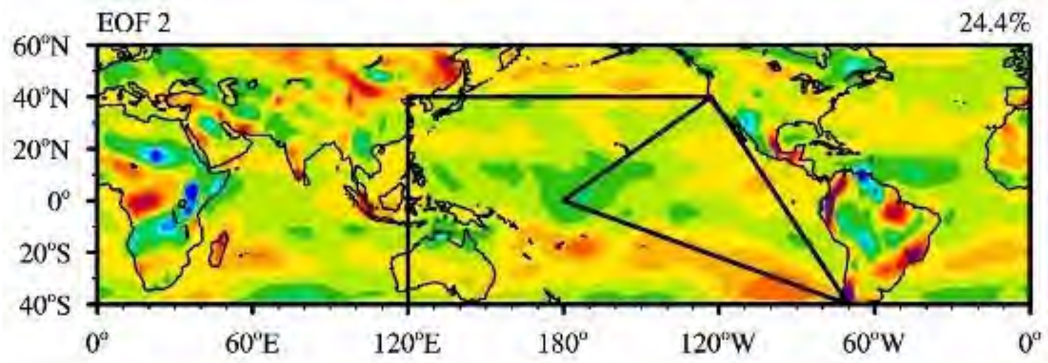

MOD

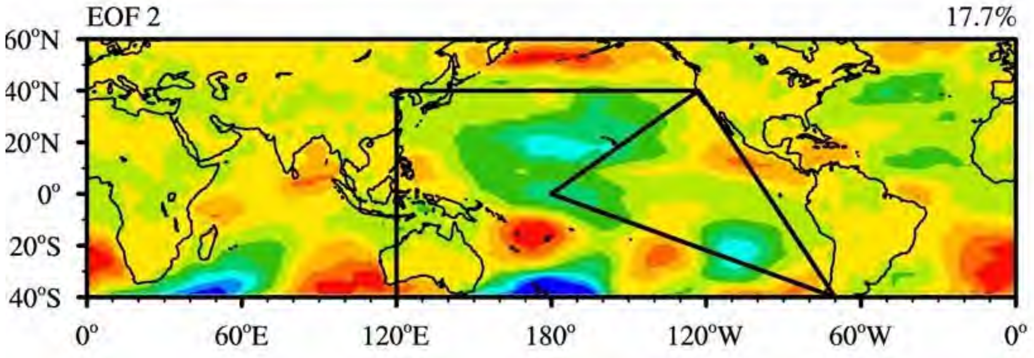

CTL

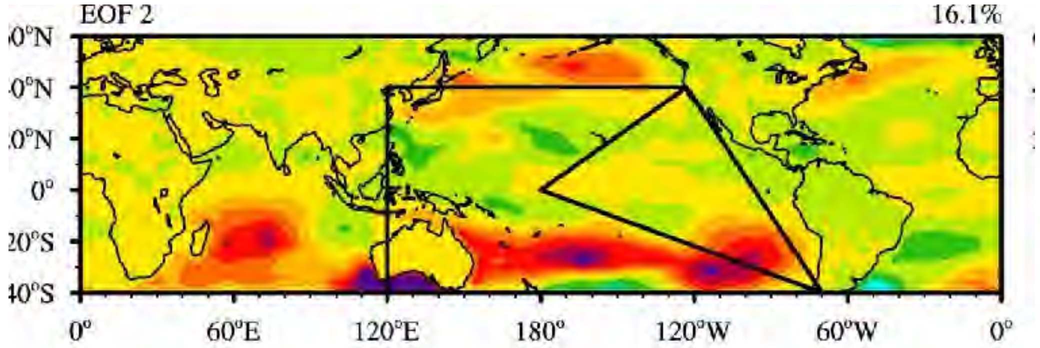

Impact of AMO on Pacific

CGCM

AMO SST forced experiment – control experiment

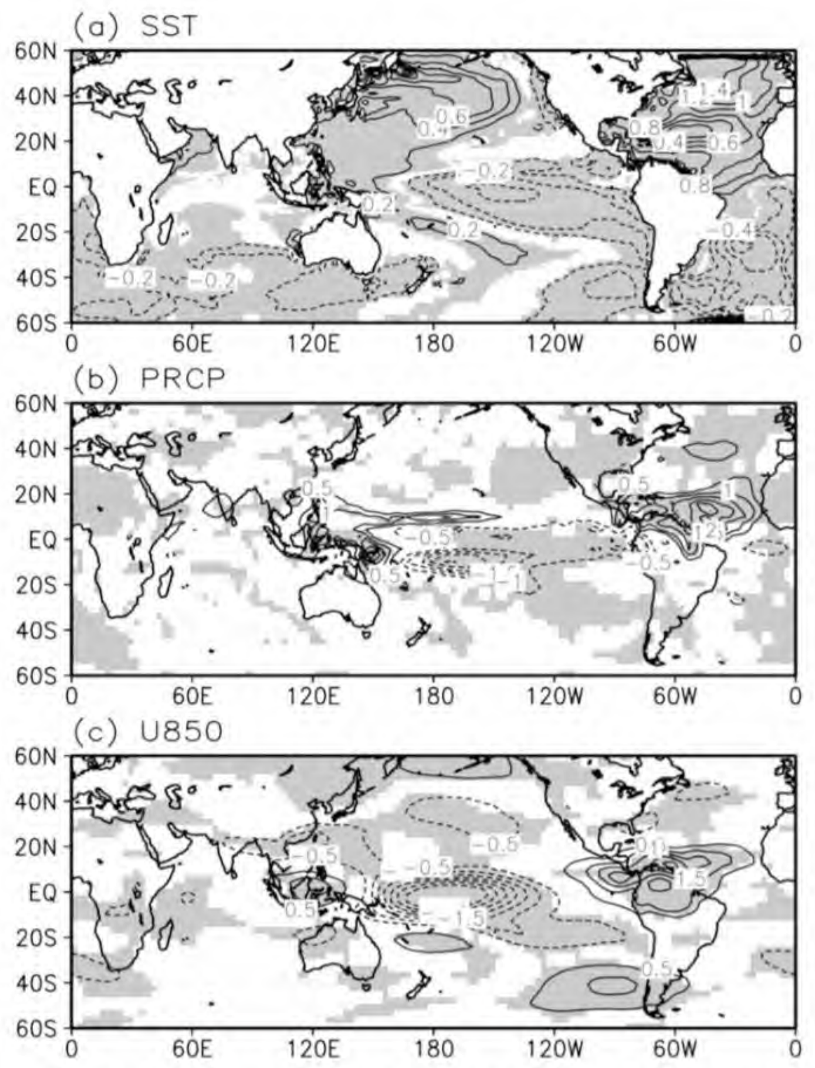

FIG. 4. Difference maps of (a) SST (°C), (b) precipitation (mm day^{-1}), and (c) 850-hPa zonal wind (m s^{-1}) between the CGCM experiments of the CNT and AMO runs. Shading indicates differences above the 95% significant level.

Kang et al. 2014

Cold SST

Less rainfall

Stronger easterly wind

AMO simulation

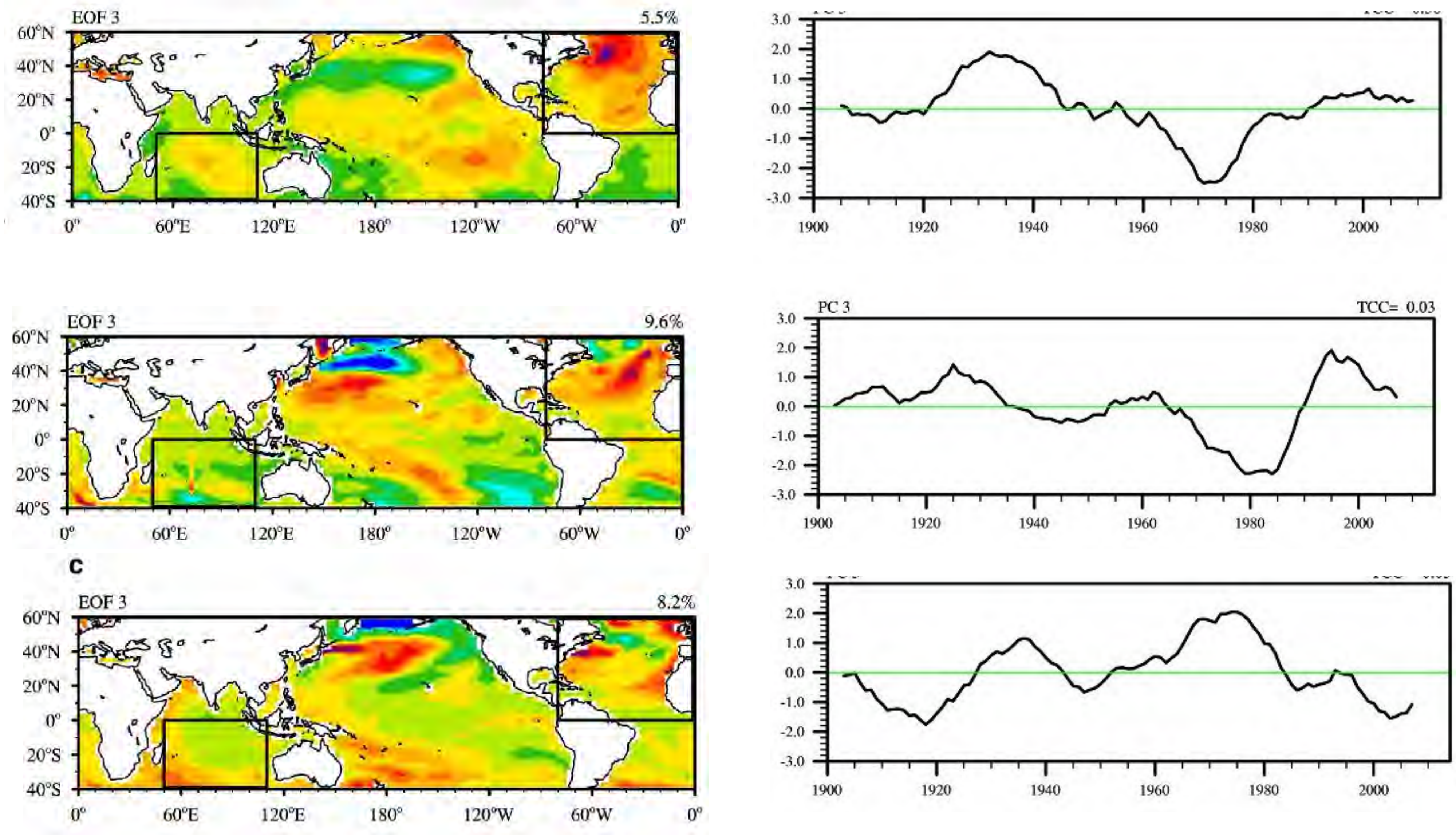

What control AMO?

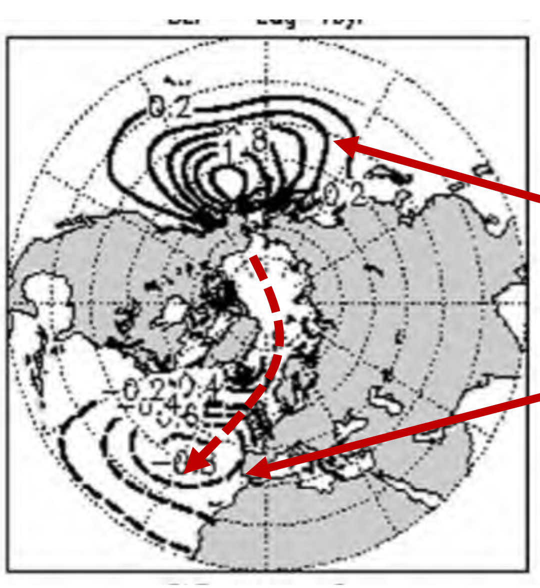

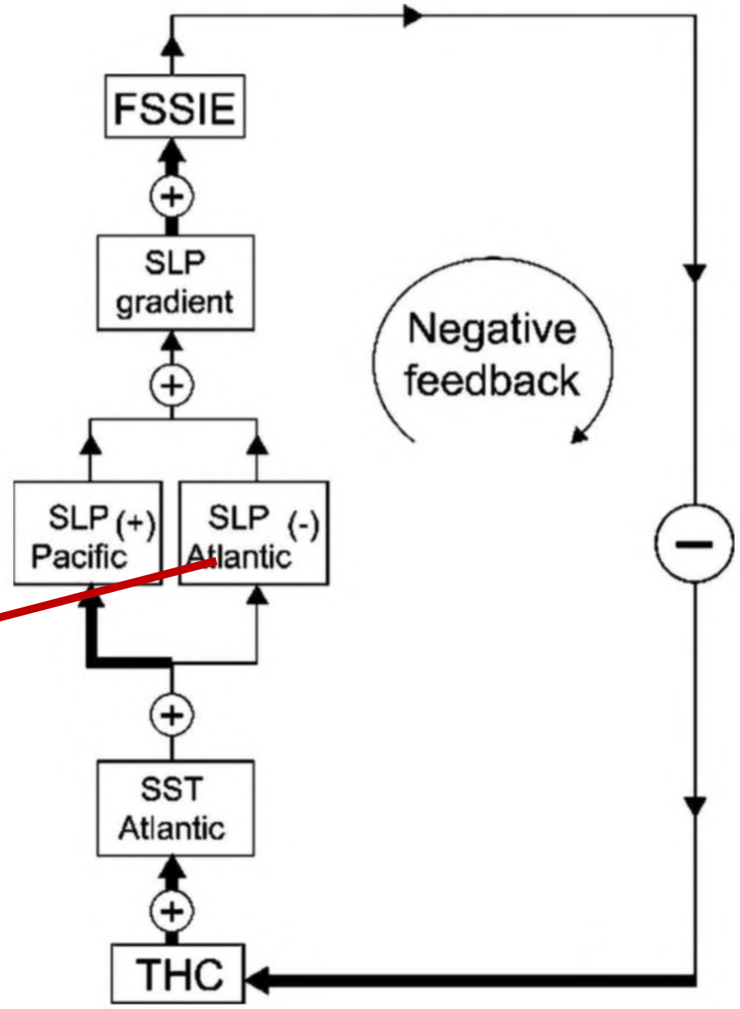

Dima & Lohmann (2006)

Decal pattern of SLP in models

MOD

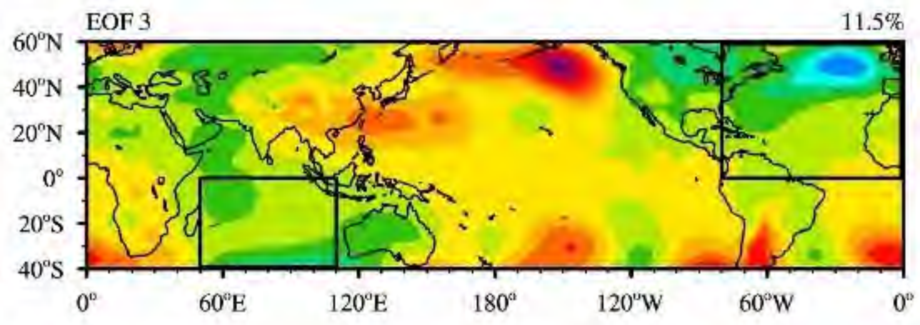

CTL

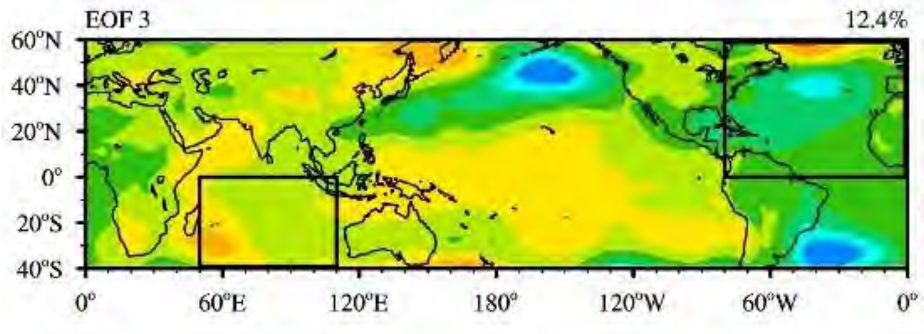

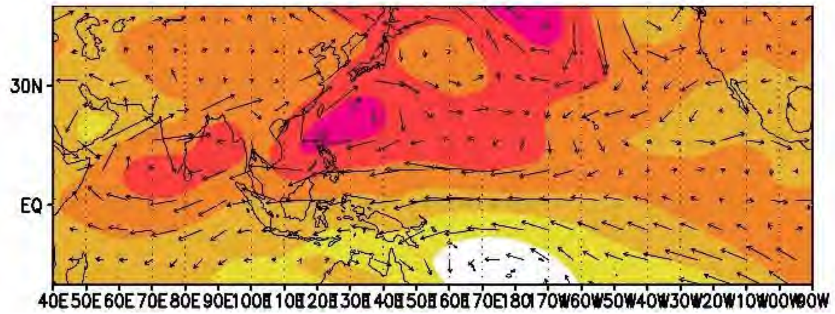

How MODIFICATIONS work

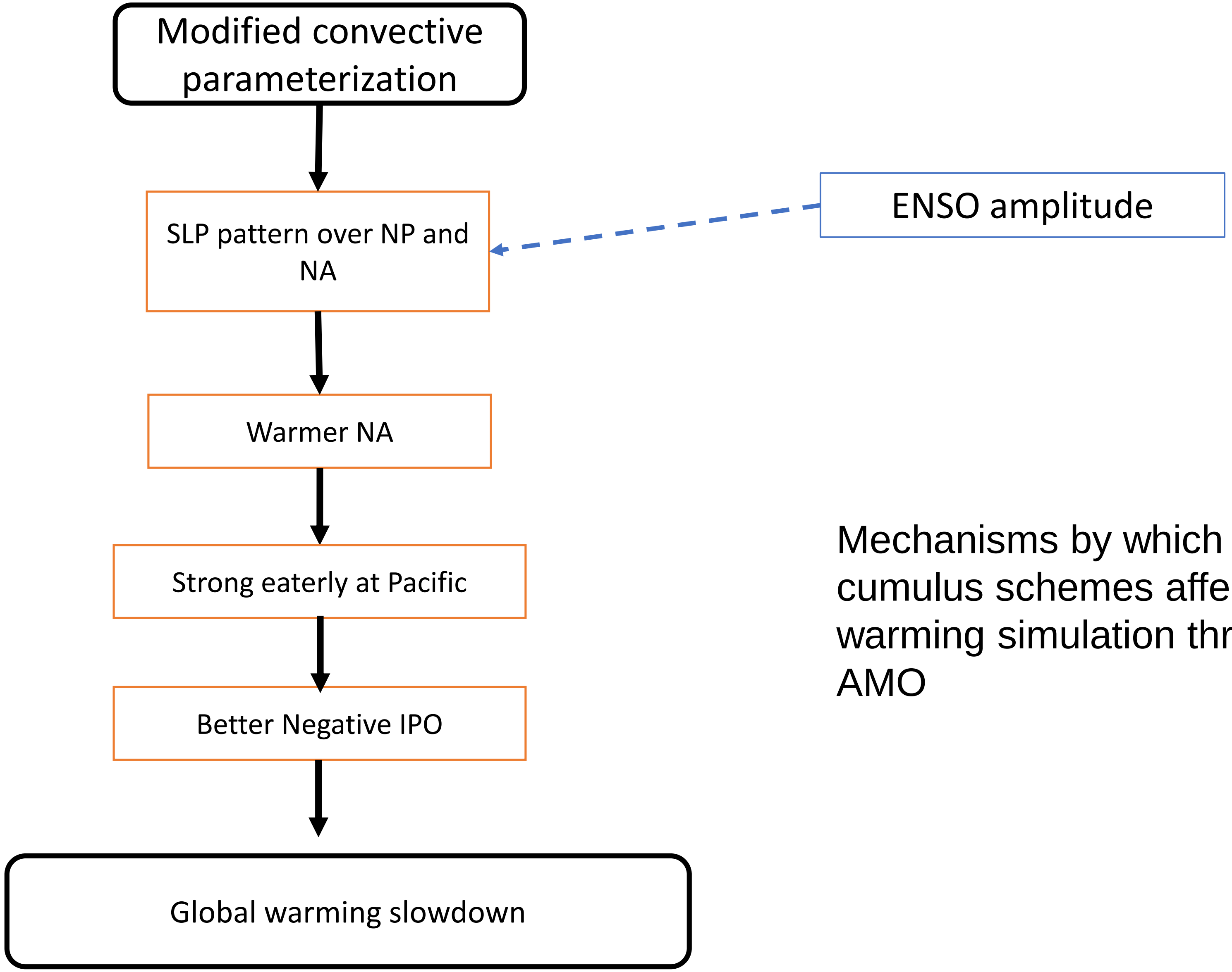

Mechanisms by which the modified cumulus schemes affect global warming simulation through IPO and AMO